

A GEOMETRY-ADAPTIVE REGULARIZED NEWTON-TYPE METHOD FOR MANIFOLD-AFFINE INTERSECTION PROBLEMS

DENGYU ZHENG* AND SHIXIANG CHEN*

Abstract. We propose Regularized Newton-SLRA (RN-SLRA), a regularized Newton-type method for local manifold–affine intersection problems motivated by structured low-rank approximation. Classical Newton-SLRA achieves fast local convergence under transversality, but its tangent-space intersection step may become ill-defined, singular, or severely ill-conditioned when transversality fails. RN-SLRA overcomes this difficulty by replacing the exact tangent-space intersection step with a regularized quadratic subproblem over the affine space. Under intrinsic transversality, we prove local linear convergence to the intersection. Under transversality, we show that a residual-dependent choice of the regularization parameter yields higher-order local convergence; in particular, the method converges quadratically for the linear residual rule. We also analyze an inexact variant based on quasioptimal manifold projections. When the quasioptimality constant is sufficiently accurate, the inexact method retains local linear residual convergence. Numerical experiments on constructed degenerate SLRA instances and Hankel-structured examples illustrate the robustness of RN-SLRA in settings where Newton-SLRA may fail, and show that the inexact variant can reduce the projection cost in large-scale problems.

Key words. Manifold–affine intersection problems, structured low-rank approximation, regularization, inexact projection, (intrinsic) transversality, local convergence

MSC codes. 65Y20, 65F55, 90C30

1. Introduction. Structured low-rank approximation (SLRA) seeks to approximate a structured matrix M by a matrix M_r with the same structure and prescribed rank. Typical structures include Hankel, Toeplitz, Sylvester, and more general affine matrix structures [11, 31]. In contrast to classical low-rank approximation, which admits an explicit solution by the SVD, SLRA must enforce the affine structure and the rank constraint simultaneously. This coupling makes the problem substantially more difficult. SLRA arises in signal processing, system identification, and computer algebra [31, 32, 23]; for example, low-rank Hankel approximation is related to exponential data fitting, frequency estimation, and denoising, while Sylvester-structured low-rank approximation is important in approximate polynomial GCD computations [31, 33, 23].

Geometrically, an affine matrix structure is represented by an affine subspace, whereas the rank constraint is represented locally by a smooth fixed-rank manifold. Thus SLRA naturally leads to a manifold–affine intersection problem. Let $\mathcal{M}_{p,q}(\mathbb{R})$ denote the space of real $p \times q$ matrices, equipped with the Frobenius inner product $\langle M_1, M_2 \rangle = \text{tr}(M_1^\top M_2)$ and norm $\|M\| = \sqrt{\text{tr}(M^\top M)}$. Denote by \mathcal{D}_r the subset of $\mathcal{M}_{p,q}(\mathbb{R})$ consisting of matrices of rank r . All local statements involving \mathcal{D}_r are understood in a neighborhood of a rank- r point $x^* \in E \cap \mathcal{D}_r$ with $\sigma_r(x^*) > 0$; in such a neighborhood, \mathcal{D}_r is a smooth fixed-rank manifold and the metric projection onto \mathcal{D}_r is locally single-valued. The local SLRA problem considered in this paper can be formulated as follows.

Problem 1.1 (SLRA). Consider an affine subspace $E \subset \mathcal{M}_{p,q}(\mathbb{R})$, a matrix $M \in E$, and an integer $r \in \{0, 1, \dots, \min(p, q)\}$. Find a matrix $M_r \in E \cap \mathcal{D}_r$ close to M .

Computing a metric projection onto $E \cap \mathcal{D}_r$ is generally difficult. In practice,

* School of Mathematical Sciences, Key Laboratory of the Ministry of Education for Mathematical Foundations and Applications of Digital Technology, University of Science and Technology of China, Hefei, Anhui, China (zq_renius919@mail.ustc.edu.cn, shxchen@ustc.edu.cn).

one usually seeks a nearby feasible point in $E \cap \mathcal{D}_r$, which can be regarded as a local approximation to the projection onto the manifold–affine intersection. Many algorithms have been proposed for this purpose. Among them, the Cadzow algorithm [8] can be viewed as an alternating-projection method between the affine structure set and the fixed-rank manifold. It is simple and robust, and converges locally linearly under separability-type intersection conditions [28, 15]. In contrast, Newton-SLRA [40] and APHL [44] are Newton-type variants with local quadratic convergence under transversality. Other approaches include structured total least squares methods [39, 37], Riemannian optimization [1, 42], alternating minimization [22], variable projection [34], gradient systems [16], and algebraic methods [36].

The quadratic convergence of Newton-SLRA, however, relies on a restrictive geometric requirement: in the SLRA setting, the affine subspace E and the fixed-rank manifold \mathcal{D}_r must intersect transversally. When transversality fails, the tangent-space intersection in the Newton-SLRA update may be empty, and the associated linear system may become singular or severely ill-conditioned. Thus, although alternating projections remain applicable under weaker intersection conditions, the fast local behavior of Newton-SLRA is no longer available. This motivates the construction of a Newton-type method that is well defined under weaker geometry and recovers fast convergence under transversality.

To address this issue, we propose Regularized Newton-SLRA (RN-SLRA) for local manifold–affine intersection problems. The method replaces the potentially ill-defined tangent-space intersection step in Newton-SLRA by a regularized subproblem over the affine space. The regularization parameter is chosen as

$$\mu_k = cr_k^\rho, \quad r_k := d_M(x_k) = \|x_k - P_M(x_k)\|, \quad c > 0, \quad \rho \in [0, 1].$$

This residual-dependent choice makes the method geometry-adaptive: the regularization stabilizes the step when the manifold residual is not small, and for $\rho > 0$ it becomes asymptotically weaker as the iterates approach the intersection. We prove local linear convergence under intrinsic transversality. Under transversality, the same choice yields local convergence of order $1 + \rho$, including quadratic convergence when $\rho = 1$. We also record a retraction interpretation of the RN-SLRA limit map under clean intersection; for fixed regularization ($\rho = 0$), the limit map defines a genuine retraction, and a second-order retraction under additional smoothness. This observation is of independent interest for optimization problems constrained to intersection manifolds [45, 10].

For large-scale SLRA problems, the projection onto the fixed-rank manifold may itself be computationally expensive. We therefore further introduce Inexact Regularized Newton-SLRA (iRN-SLRA), which replaces the exact manifold projection by a σ -quasioptimal projection [7]. The inexact variant preserves the local convergence rates of RN-SLRA under the corresponding intersection assumptions, while allowing cheaper projection computations. The local convergence properties of the methods discussed above are summarized in Table 1.

We evaluate RN-SLRA and iRN-SLRA on constructed degenerate SLRA instances and low-rank Hankel approximation problems at both small and large scales. The numerical results are consistent with the theoretical motivation above: on instances where transversality fails, RN-SLRA remains convergent, whereas Newton-SLRA may diverge. In addition, iRN-SLRA exhibits convergence behavior comparable to that of RN-SLRA while reducing the computational cost of the manifold projection step, with more pronounced savings on large-scale problems.

TABLE 1

Local convergence rates of representative methods under different intersection conditions.

	Intrinsic transversality	Transversality
Cadzow (AP)	linear	linear
Newton-SLRA	–	quadratic
RN-SLRA (ours)	linear	order $1 + \rho$; quadratic if $\rho = 1$
iRN-SLRA (ours)	linear	order $1 + \rho$; quadratic if $\rho = 1$

2. Preliminaries. We consider the general problem of approximating the projection of a point x onto the intersection $X := M \cap E$ of a smooth embedded manifold M and an affine subspace E in a Euclidean space, assuming without loss of generality that $M \neq E$; in particular, the SLRA problem is recovered when $M = \mathcal{D}_r$.

2.1. Notations and Basic Facts. We use $d_C(x)$ to denote the distance from x to the set C , and $P_C(x)$ to represent the projection of x onto the set C . $B(x, r)$ denotes the ball centered at x with radius r . We use $\hat{u} = \frac{u}{\|u\|}$ to represent the unit vector of u . For any affine subspace A , let A^0 denote its underlying vector space, so that $A = x + A^0$ for any $x \in A$. In particular, we write $E = x + L$ for any $x \in E$, where $L := E^0$. For an affine manifold V and a point $x \in V$, we denote by $T_x V$ the affine tangent space of V at x , and by $N_x V$ the affine normal space of V at x . Their underlying vector spaces are denoted by $T_x V^0$ and $N_x V^0$. L^\perp denotes the orthogonal complement of L .

Assumption 2.1. E is an affine subspace and M is a smooth manifold of class C^2 .

We first recall some intersection conditions, including the transversality condition [28, 20, 21], the clean intersection condition [4], the intrinsic transversality condition [13, 14], the separability condition [35], and the subtransversality condition [24].

DEFINITION 2.2 (Transversality). *Let \mathbb{E} be a Euclidean space. Let $M \subset \mathbb{E}$ be a manifold of class C^1 and let E be an affine subspace of \mathbb{E} . We say that E intersects M transversally at a point $\bar{x} \in X$ if $\text{codim}(L \cap T_{\bar{x}} M^0) = \text{codim}(L) + \text{codim}(T_{\bar{x}} M^0)$.*

We have the following lemma under transversality:

LEMMA 2.3 (Uniform angle bound under transversality). *Assume that E and M intersect transversally at \bar{x} . Then, after possibly shrinking the neighborhood of \bar{x} , there exists a constant $\eta > 0$ such that, for every $y \in M$ sufficiently close to \bar{x} and every $n \in N_y M^0$,*

$$(2.1) \quad \|P_L n\| \geq \eta \|n\|.$$

This lemma follows from [40, lemma 4.5]. A proof can be found in [12, lemma 9.5].

DEFINITION 2.4 (Clean intersection). *Let \mathbb{E} be a Euclidean space. Let $M \subset \mathbb{E}$ be a manifold of class C^p ($p \geq 2$) and let E be an affine subspace of \mathbb{E} . We say that E intersects M cleanly at a point $\bar{x} \in X$ if the set X is a C^p embedded submanifold and $T_x X = T_x M \cap L$ for all $x \in X$ sufficiently close to \bar{x} .*

DEFINITION 2.5 (Intrinsic Transversality). *Let \mathbb{E} be a Euclidean space. Let $M \subset \mathbb{E}$ be a manifold of class C^1 and let E be an affine subspace of \mathbb{E} . We say that E intersects M intrinsically transversally at a point $\bar{x} \in X$ if there exists a constant $\kappa > 0$ such that for all $x \in E \setminus M$ and $y \in M \setminus E$ sufficiently close to \bar{x} ,*

$$\max \left\{ d \left(\widehat{x - y}, N_y M^0 \right), d \left(\widehat{x - y}, N_x E^0 \right) \right\} \geq \kappa.$$

DEFINITION 2.6 (Separability). *Let \mathbb{E} be a Euclidean space. Let $M \subset \mathbb{E}$ be a manifold of class C^1 and let E be an affine subspace of \mathbb{E} . We say that E intersects M separably at a point $\bar{x} \in X$ if there exists an angle $\alpha > 0$ such that for any point $z \in E \setminus M$ sufficiently close to \bar{x} , and any points $x \in P_M(z) \setminus E$ and $z' \in P_E(x)$, the angle between the vectors $z - x$ and $z' - x$ is at least α .*

The notion of separability was introduced in [35] under the term 0-separability. This property is particularly suitable for the analysis of alternating projections and inexact alternating projection methods [15]. In our work, intrinsic transversality serves as the main geometric assumption for the local linear convergence analysis.

Assumption 2.7. E intersects M intrinsically transversally at \bar{x} .

Under Assumption 2.1, intrinsic transversality is equivalent to separability in either order; see Lemma 2.8 below. Although separability is not symmetric in general, in the present C^2 manifold–affine setting the two directional versions are equivalent. More precisely, E intersects M separably at \bar{x} if and only if M intersects E separably at \bar{x} , and these are both equivalent to intrinsic transversality.

LEMMA 2.8. *Let \mathbb{E} be a Euclidean space, let $M \subset \mathbb{E}$ be a C^2 manifold, and let $E \subset \mathbb{E}$ be an affine subspace. Then the following are equivalent at $\bar{x} \in E \cap M$:*

- (1) E intersects M separably at \bar{x} ;
- (2) M intersects E separably at \bar{x} ;
- (3) E intersects M intrinsically transversally at \bar{x} .

Proof. Write $E = \bar{x} + L$, so $N_x E = L^\perp$ for all $x \in E$.

(1) \Rightarrow (2). Assume that E intersects M separably at \bar{x} . After possibly shrinking U , we may assume that $P_E(M \cap U) \subset U$ and $P_M(E \cap U) \subset U$ by continuity of P_E at \bar{x} and local single-valuedness and continuity of P_M near \bar{x} .

Take $y \in (M \cap U) \setminus E$, $x = P_E(y) \in U \setminus M$, $y^+ \in P_M(x) \cap U$, and set $x^+ := P_E(y^+)$. If $y^+ \in E$, then $y^+ - x \in L$, $y - x \in L^\perp$, hence $\angle(y - x, y^+ - x) = \frac{\pi}{2} \geq \alpha$. Assume now $y^+ \notin E$. Since $x \in E$, $y^+ \in P_M(x) \setminus E$, and $x^+ = P_E(y^+)$, separability gives $\angle(x - y^+, x^+ - y^+) \geq \alpha$. Moreover, $x^+ - y^+ = P_{L^\perp}(x - y^+)$ and $x - y \in L^\perp$. By Cauchy's inequality, among all nonzero vectors $w \in L^\perp$, the angle between $x - y^+$ and w is minimized when w is parallel to $P_{L^\perp}(x - y^+)$. Hence $\angle(x - y^+, x - y) \geq \angle(x - y^+, x^+ - y^+) \geq \alpha$. Equivalently, $\angle(y - x, y^+ - x) \geq \alpha$. Thus M intersects E separably at \bar{x} .

(2) \Rightarrow (3). Assume that M intersects E separably at \bar{x} , but intrinsic transversality fails. Then there exist $a_k \in E \setminus M$, $y_k \in M \setminus E$, $a_k \rightarrow \bar{x}$, $y_k \rightarrow \bar{x}$, such that, with $w_k := \widehat{y_k - a_k}$,

$$\max\{d(w_k, L^\perp), d(w_k, N_{y_k} M^0)\} \rightarrow 0.$$

Set $x_k := P_E(y_k)$, $t_k := \|y_k - x_k\|$, $u_k := \frac{y_k - x_k}{\|y_k - x_k\|}$. Then $u_k \in L^\perp$ and $P_{L^\perp}(y_k - a_k) = y_k - x_k$, $P_{L^\perp} w_k = \frac{t_k}{\|y_k - a_k\|} u_k$. Since $d(w_k, L^\perp) \rightarrow 0$, we have $\|P_{L^\perp} w_k\| \rightarrow 1$, hence $u_k = \frac{P_{L^\perp} w_k}{\|P_{L^\perp} w_k\|} \rightarrow w_k$. Choose $v_k \in N_{y_k} M^0$ with $\|v_k - w_k\| = d(w_k, N_{y_k} M^0) \rightarrow 0$. Then $\|u_k - v_k\| \rightarrow 0$. Define $z_k := y_k - t_k v_k$. Since M is a C^2 manifold, for all large k , z_k lies in a tubular neighborhood of M and $P_M(z_k) = y_k$. Moreover, P_M is locally Lipschitz there. As $x_k = y_k - t_k u_k$, $z_k - x_k = t_k(u_k - v_k)$, we obtain

$$\|z_k - x_k\| = t_k \|u_k - v_k\| = o(t_k), \quad \|z_k - y_k\| = t_k.$$

Hence, for all large k , necessarily $x_k \notin M$; otherwise x_k would be closer to z_k than y_k , contradicting $P_M(z_k) = y_k$.

Now let $y_k^+ := P_M(x_k)$. By local Lipschitz continuity of P_M ,

$$\|y_k^+ - y_k\| = \|P_M(x_k) - P_M(z_k)\| \leq C\|x_k - z_k\| = o(t_k).$$

Since $\|y_k - x_k\| = t_k$, it follows that $\|(y_k^+ - x_k) - (y_k - x_k)\| = o(t_k)$, and therefore $\angle(y_k - x_k, y_k^+ - x_k) \rightarrow 0$. But for all large k , $y_k \in M \setminus E$, $x_k = P_E(y_k) \in E \setminus M$, $y_k^+ \in P_M(x_k)$, so separability of M relative to E yields some $\alpha_0 > 0$ such that $\angle(y_k - x_k, y_k^+ - x_k) \geq \alpha_0$, a contradiction. Hence E and M are intrinsically transversal at \bar{x} .

(3) \Rightarrow (1). This follows from the fact that intrinsic transversality implies separability; see [35, Proposition 2]. Therefore (1), (2), and (3) are equivalent. \square

DEFINITION 2.9 (Subtransversality). *Let \mathbb{E} be a Euclidean space. Let $M \subset \mathbb{E}$ be a manifold of class C^1 and let E be an affine subspace of \mathbb{E} . We say that E intersects M subtransversally at a point $\bar{x} \in X$ if there exist constants $\tau > 0$ and a neighborhood U of \bar{x} such that for all $w \in U$,*

$$d(w, X) \leq \tau (d(w, E) + d(w, M)).$$

Under the present C^2 embedded manifold–affine setting and with the definitions used here, the following relationships hold locally, rather than as unconditional statements for arbitrary sets: transversality implies clean intersection; clean intersection is equivalent to intrinsic transversality [45, Theorem 5.1]; intrinsic transversality implies subtransversality; and intrinsic transversality is equivalent to separability in either order; see [14, 35, 45].

2.2. Cadzow Algorithm. The alternating projection (AP) method has a long history [41, 43]. Recent studies have analyzed AP and inexact AP methods for various sets [5, 27, 25], together with their local linear convergence properties [27, 35, 30, 15]. In the context of structured low-rank approximation, the Cadzow algorithm [8, 18] can be viewed as an alternating projection method between the affine space E and the low-rank manifold M . More precisely, starting from $x_k \in E$, one step of the Cadzow iteration is given by

$$(2.2) \quad x_{k+1} = P_E P_M(x_k).$$

In the local rank- r neighborhood considered in this paper, it is well known that the projection onto \mathcal{D}_r can be computed by the truncated SVD.

LEMMA 2.10 (Eckart-Young Theorem). *Let $x \in \mathcal{M}_{p,q}(\mathbb{R})$ be a matrix, and let r be a positive integer not greater than $\min(p, q)$. Let $x = USV^\top$ be its SVD, where $S = \text{diag}(\sigma_1, \dots, \sigma_{\min(p,q)})$ with $\sigma_1 \geq \dots \geq \sigma_{\min(p,q)} \geq 0$. If x is sufficiently close to a rank- r point x^* with $\sigma_r(x^*) > 0$, then a projection $P_{\mathcal{D}_r}(x)$ is given by*

$$P_{\mathcal{D}_r}(x) = U\tilde{S}V^\top, \quad \tilde{S} = \text{diag}(\sigma_1, \dots, \sigma_r, 0, \dots, 0).$$

Then the Cadzow algorithm can be formulated as:

$$(2.3) \quad \begin{aligned} U, S, V &\leftarrow \text{SVD}(x_k), & y_k &= U_r S_r V_r^\top, \\ x_{k+1} &= x_k + \sum_{i=1}^d \langle y_k - x_k, E_i \rangle E_i. \end{aligned}$$

where U_r denotes the matrix consisting of the first r columns of U , V_r denotes the matrix consisting of the first r columns of V , S_r denotes the $r \times r$ top-left submatrix

of S , d is the dimension of E , and $\{E_i\}_{i=1}^d$ denotes an orthonormal basis of L . The update formula for x_{k+1} is obtained by

$$x_{k+1} = P_E(y_k) = x_k + P_L(y_k - x_k).$$

If E intersects M transversally at $\bar{x} \in X$ and the initial point is sufficiently close to \bar{x} , the Cadzow algorithm converges locally linearly to a point $x_\infty \in X$ [28]. In fact, local linear convergence can already be guaranteed when E intersects M separably [15].

2.3. Newton-SLRA Algorithm. The Newton-SLRA algorithm is motivated by Newton's method. In each iteration of the classical Newton-SLRA, given the current iterate $x_k \in E$, one first computes its projection onto the manifold $y_k = P_M(x_k)$, and then solves a linear least-squares problem: $x_{k+1} = P_{E \cap T_{y_k} M}(x_k)$, i.e., the closest point to x_k in the intersection of E and the tangent space $T_{y_k} M$. Under the transversality condition, this algorithm converges locally quadratically. When $M = \mathcal{D}_r$, the algorithm can be formulated as:

$$(2.4) \quad \begin{aligned} U, S, V &\leftarrow \text{SVD}(x_k), & y_k &= U_r S_r V_r^\top, \\ N_{ij} &\leftarrow u_i v_j^\top, & i &= r+1, \dots, p, \quad j = r+1, \dots, q, \\ A &\leftarrow (\langle N_{ij}, E_\ell \rangle)_{(i,j),\ell}, & b &\leftarrow (\langle N_{ij}, y_k - x_k \rangle)_{(i,j)}, \\ x_{k+1} &= x_k + \sum_{\ell=1}^d (A^\dagger b)_\ell E_\ell. \end{aligned}$$

However, when transversality fails, the matrix A in (2.4) may lose rank at the solution. In the fixed-rank SLRA setting, full row rank of the tangent-space linear system is equivalent to transversality of E and \mathcal{D}_r at the intersection point. Hence, near a nontransversal solution, the associated least-squares problem may become singular or severely ill-conditioned.

Another issue is that the well-definedness of Newton-SLRA relies on the non-emptiness of $E \cap T_{y_k} M$. Under transversality, there exists a positive lower bound α for the angle between E and $T_{y_k} M$ in some neighborhood of \bar{x} , but this cannot be guaranteed under intrinsic transversality, as $E \cap T_{y_k} M$ may be empty.

These issues motivate the regularized modification introduced below.

3. Regularized Newton-SLRA. We introduce a regularization term and define the next iterate as:

$$(3.1) \quad \begin{aligned} y_k &= P_M(x_k), \\ x_{k+1} &= \arg \min_{x \in E} \left\{ \frac{1}{2} \|x - y_k\|^2 + \frac{1}{2\mu_k} \|P_{N_{y_k} M}(x - y_k)\|^2 \right\}, \quad \mu_k > 0. \end{aligned}$$

where $P_{N_{y_k} M}$ is the orthogonal projector onto the normal space $N_{y_k} M$, and μ_k is a regularization parameter. In the algorithm studied below, μ_k is chosen adaptively according to:

$$\mu_k = c \cdot r(x_k)^\rho, \quad r(x_k) = \|x_k - y_k\| = d_M(x_k).$$

where $c > 0$ is a constant, $0 \leq \rho \leq 1$ is a parameter. This choice of the regularization parameter is inspired by the residual-dependent regularization strategy used in the Inexact Regularized Proximal Newton method (IRPN) [47], and is also related to earlier regularized Newton methods for convex minimization with singular solutions

Algorithm 3.1 Regularized Newton-SLRA (RN-SLRA)

-
- 1: **Input:** Initial point $x_0 \in E$, parameters $c > 0$ and $0 \leq \rho \leq 1$
 - 2: Write $E = x_0 + L$, where $L = E^0$, and fix an orthonormal basis $\{e_1, \dots, e_d\}$ of L
 - 3: **for** $k = 0, 1, 2, \dots$ **do**
 - 4: Compute an SVD $x_k = U\Sigma V^\top$ and set $y_k := U_r \Sigma_r V_r^\top \in P_{\mathcal{D}_r}(x_k)$.
 - 5: Set $r(x_k) := \|x_k - y_k\|$. Set $\mu_k := c r(x_k)^\rho$. Set $b_k := x_k - y_k$.
 - 6: For $a = r + 1, \dots, m$ and $b = r + 1, \dots, n$, define $N_{ab} := u_a v_b^\top$
 - 7: Form A_k, β_k , and η_k by $(A_k)_{(a,b),i} = \langle N_{ab}, e_i \rangle$, $(\beta_k)_i = \langle b_k, e_i \rangle$, and $(\eta_k)_{(a,b)} = \langle N_{ab}, b_k \rangle$.
 - 8: Solve $(I_d + \mu_k^{-1} A_k^\top A_k) \alpha^{(k)} = -\beta_k - \mu_k^{-1} A_k^\top \eta_k$.
 - 9: Set $x_{k+1} := x_k + \sum_{i=1}^d \alpha_i^{(k)} e_i$
 - 10: **end for**
-

[29] as well as improved proximal Newton implementations such as newGLMNET [46].

Since E is affine, the objective function in (3.1) for solving x_{k+1} is a strongly convex quadratic problem with a unique solution, which can be obtained by solving a linear system. Thus, the well-definedness of the RN-SLRA step does not require the transversality condition between E and M .

3.1. Derivation of the Linear System. Let $\{E_1, \dots, E_d\}$ be an orthonormal basis of L , set $b = x_k - y_k$, and write $N = N_{y_k} M$. Choose an orthonormal basis $\{N_j\}_{j=1}^s$ of N . Since $E = x_k + L$, any $x \in E$ can be written as $x = y_k + b + \sum_{i=1}^d \alpha_i E_i$. Substituting this expression into (3.1) and using the first-order optimality condition gives

$$(3.2) \quad \left(I_d + \frac{1}{\mu_k} A^\top A \right) \alpha = -\beta - \frac{1}{\mu_k} A^\top \eta,$$

where $A_{ji} = \langle N_j, E_i \rangle$, $\eta_j = \langle N_j, b \rangle$, and $\beta_i = \langle b, E_i \rangle$. Since $A^\top A \succeq 0$ and $\mu_k > 0$, the coefficient matrix is positive definite. The next iterate is $x_{k+1} = x_k + \sum_{i=1}^d \alpha_i E_i$.

For the fixed-rank manifold $M = \mathcal{D}_r$, this yields Algorithm 3.1.

3.2. Limiting Interpretation of the Regularized Step. Assume that E and M intersect transversally at \bar{x} , so that $E \cap T_{y_k} M$ is nonempty for y_k sufficiently close to \bar{x} . The role of μ_k can be understood from two limiting regimes.

If $\mu_k \rightarrow \infty$, the penalty term vanishes and the subproblem reduces to $\min_{x \in E} \|x - y_k\|^2$. Hence the step becomes $p_k = P_E(y_k)$, namely the alternating projection step. If $\mu_k \rightarrow 0$, the penalty term enforces $P_{N_{y_k} M}(x - y_k) = 0$, or equivalently $x \in T_{y_k} M$. Thus the limiting problem is $\min_{x \in E \cap T_{y_k} M} \|x - y_k\|^2$. Since $y_k = P_M(x_k)$, we have $x_k - y_k \in N_{y_k}^0 M$. Hence, for every $x \in T_{y_k} M$, $\|x - x_k\|^2 = \|x - y_k\|^2 + \|x_k - y_k\|^2$. Therefore, minimizing the distance to y_k over $E \cap T_{y_k} M$ is equivalent to minimizing the distance to x_k over the same set. The limiting step is the Newton-SLRA point $q_k = P_{E \cap T_{y_k} M}(x_k)$, provided that $E \cap T_{y_k} M$ is nonempty.

Thus, for $\mu_k \in (0, \infty)$, the regularized step interpolates between alternating projections and Newton-SLRA: smaller μ_k gives a more Newton-like step, while larger μ_k gives a more projection-like step. This interpretation relies on the local nonemptiness of $E \cap T_{y_k} M$, which follows from transversality but may fail under Assumption 2.7; it is used only as intuition and not in the convergence analysis below.

3.3. Inexact Regularized Newton-SLRA. We replace $y_k = P_M(x_k)$ in (3.1) by a quasioptimal projection and obtain iRN-SLRA:

$$(3.3) \quad \begin{aligned} & y_k \in M \text{ such that } \|x_k - y_k\| \leq \sigma d_M(x_k), \quad \sigma \geq 1, \\ & x_{k+1} = \arg \min_{x \in E} \left\{ \frac{1}{2} \|x - y_k\|^2 + \frac{1}{2\mu_k} \|P_{N_{y_k}M}(x - y_k)\|^2 \right\}, \quad \mu_k > 0. \end{aligned}$$

When $\sigma = 1$, iRN-SLRA reduces to RN-SLRA. For $\sigma > 1$, y_k is a σ -quasioptimal projection of x_k onto M , in the sense of [7]. This quasioptimal model is well suited to low-rank approximation: truncated SVD gives the exact projection with $\sigma = 1$, while randomized SVD provides a practical approximate rank- r projection, with residual error bounds available in expectation or with high probability under standard randomized low-rank approximation results [19]; partial SVD can also be used in practice [26]. Compared with a full SVD, these approaches can significantly reduce the computational cost, especially for large-scale problems.

For an $m \times n$ rank- r SLRA problem with affine dimension d , one RN-SLRA iteration consists of: (i) computing the rank- r projection, implemented by a truncated or full SVD; (ii) forming the normal-coordinate matrix $A_k \in \mathbb{R}^{(m-r)(n-r) \times d}$; and (iii) solving a $d \times d$ symmetric positive definite linear system. Thus the dominant cost is typically the rank- r projection and the construction of A_k , while the $d \times d$ solve is moderate when d is small or structured. For Hankel/Toeplitz structures, the affine basis and matrix-vector products can often be represented implicitly, and randomized or partial SVD can reduce the projection cost in large-scale settings.

4. Local Convergence Analysis. In this section, we establish the local convergence properties of the proposed algorithms. We first prove that RN-SLRA converges linearly under intrinsic transversality. We then show that, under the stronger transversality condition, the convergence rate improves to higher-order convergence, including quadratic convergence when $\rho = 1$. Finally, we extend the analysis to the inexact variant iRN-SLRA. Throughout this section, $\{x_k\}$ denotes the sequence of iterates generated by the corresponding algorithm.

4.1. Linear Convergence of RN-SLRA under Intrinsic Transversality.

LEMMA 4.1. *Suppose that Assumptions 2.1 and 2.7 hold. There exist constants $\delta_1 > 0$ and $\kappa > 0$ such that, for every $y \in M \cap B(\bar{x}, \delta_1)$, $d_X(y) \leq \kappa d_E(y)$.*

LEMMA 4.2. *Suppose that Assumptions 2.1 and 2.7 hold. There exist constants $\delta_2 > 0$ and $\kappa' > 0$ such that, for every $x \in E \cap B(\bar{x}, \delta_2)$, $d_X(x) \leq \kappa' d_M(x)$.*

Both of the above lemmas can be derived from subtransversality, which itself follows from intrinsic transversality. These two lemmas show that there exists a neighborhood U of \bar{x} such that the distance from a point in $E \cap U$ to M , or from a point in $M \cap U$ to E , is of the same order as its distance to X .

PROPOSITION 4.3 (Second-order normal estimates near a C^2 manifold). *Suppose that Assumption 2.1 holds. Then, after possibly shrinking the neighborhood of \bar{x} , there exist constants $\eta, G, G' > 0$ such that the following hold for all points sufficiently close to \bar{x} :*

(1) for all $y, z \in M$,

$$(4.1) \quad \|P_{N_y M^0}(z - y)\| \leq \eta \|z - y\|^2;$$

(2) for all $y \in M$ and all x sufficiently close to y ,

$$(4.2) \quad d_M(x) \leq \|P_{N_y M^0}(x - y)\| + G \|x - y\|^2;$$

(3) for all $y \in M$ and all x sufficiently close to y ,

$$(4.3) \quad \|P_{N_y M^0}(x - y)\| \leq d_M(x) + G' \|x - y\|^2.$$

Proof. By the local C^2 geometry of M , for each $y \in M$ near \bar{x} and each $u \in T_y M^0$ small, points of M near y can be represented as $y + u + v_y(u)$ with $v_y(u) \in N_y M^0$. Here $v_y(0) = 0$ and $Dv_y(0) = 0$; equivalently, after shrinking the neighborhood, $\|v_y(u)\| \leq c\|u\|^2$ uniformly for y near \bar{x} ; see [3, Lemma 20]. Therefore, if $z \in M$ is close to y and $u = P_{T_y M^0}(z - y)$, then $z - y = u + v_y(u)$, so $P_{N_y M^0}(z - y) = v_y(u)$, which gives (4.1).

Next, for x close to y , let $u = P_{T_y M^0}(x - y)$ and set $w := y + u + v_y(u) \in M$. Then $x - w = P_{N_y M^0}(x - y) - v_y(u)$, and hence

$$d_M(x) \leq \|x - w\| \leq \|P_{N_y M^0}(x - y)\| + c\|u\|^2 \leq \|P_{N_y M^0}(x - y)\| + c\|x - y\|^2,$$

which proves (4.2).

Finally, let $p := P_M(x)$. Since the metric projection onto M is single-valued near M [28, Lemma 2.1], applying (4.1) to $y, p \in M$ yields $\|P_{N_y M^0}(p - y)\| \leq \eta\|p - y\|^2$. Thus

$$\|P_{N_y M^0}(x - y)\| \leq \|P_{N_y M^0}(x - p)\| + \|P_{N_y M^0}(p - y)\| \leq d_M(x) + \eta\|p - y\|^2.$$

Since $\|p - y\| \leq \|p - x\| + \|x - y\| \leq 2\|x - y\|$, (4.3) follows. \square

LEMMA 4.4 (Step-size estimate). *Suppose that Assumptions 2.1 and 2.7 hold. There exist $\delta_3 > 0$ and $C_1 > 0$ such that, for all iterates $x_k \in E \cap B(\bar{x}, \delta_3)$,*

$$\|x_{k+1} - x_k\| \leq C_1 r(x_k).$$

Proof. Let $r_k := r(x_k) = d_M(x_k)$, $y_k := P_M(x_k)$. Since $x_k \in E$, we have $d_E(y_k) \leq \|y_k - x_k\| = r_k$. Hence, by Lemma 4.1, after shrinking the neighborhood if necessary, there exists $\kappa > 0$ such that $d_X(y_k) \leq \kappa d_E(y_k) \leq \kappa r_k$. Choose $z_k \in P_X(y_k)$. Then

$$(4.4) \quad \|z_k - y_k\| = d_X(y_k) \leq \kappa r_k.$$

Now define the regularized objective

$$\Phi_k(x) := \frac{1}{2}\|x - y_k\|^2 + \frac{1}{2\mu_k}\|P_{N_{y_k} M}(x - y_k)\|^2, \quad x \in E.$$

By construction, x_{k+1} minimizes Φ_k over E , so

$$(4.5) \quad \Phi_k(x_{k+1}) \leq \Phi_k(z_k).$$

Next we estimate the normal component of $z_k - y_k$. Since M is a C^2 manifold near \bar{x} (by Assumption 2.1), applying (4.1) with $y = y_k$ and $z = z_k$ and using (4.4), one has

$$(4.6) \quad \|P_{N_{y_k} M}(z_k - y_k)\| \leq \eta\|z_k - y_k\|^2 \leq \eta\kappa^2 r_k^2.$$

Therefore,

$$\Phi_k(z_k) = \frac{1}{2}\|z_k - y_k\|^2 + \frac{1}{2\mu_k}\|P_{N_{y_k} M}(z_k - y_k)\|^2 \leq \frac{1}{2}\kappa^2 r_k^2 + \frac{1}{2\mu_k}\eta^2 \kappa^4 r_k^4.$$

Using $\mu_k = cr_k^\rho$ with $c > 0$ and $0 \leq \rho \leq 1$, we get

$$(4.7) \quad \Phi_k(z_k) \leq \frac{1}{2}\kappa^2 r_k^2 + \frac{\eta^2 \kappa^4}{2c} r_k^{4-\rho}.$$

Since $4 - \rho \geq 3 > 2$, after shrinking the neighborhood further we may assume $r_k \leq 1$, and hence $\Phi_k(z_k) \leq Cr_k^2$ for some constant $C > 0$ independent of k .

Since the second term in Φ_k is nonnegative, this bound and (4.5) imply $\frac{1}{2}\|x_{k+1} - y_k\|^2 \leq \Phi_k(x_{k+1}) \leq Cr_k^2$, and therefore

$$(4.8) \quad \|x_{k+1} - y_k\| \leq \sqrt{2C} r_k.$$

Finally, by the triangle inequality,

$$\|x_{k+1} - x_k\| \leq \|x_{k+1} - y_k\| + \|y_k - x_k\| \leq \sqrt{2C} r_k + r_k = (1 + \sqrt{2C}) r_k.$$

Thus the conclusion holds with $C_1 := 1 + \sqrt{2C}$. This proves the lemma. \square

LEMMA 4.5 (Residual contraction). *Suppose that Assumptions 2.1 and 2.7 hold. There exist $\delta > 0$, $q \in (0, 1)$, and $C_2 > 0$ such that, for all $x_k \in E \cap B(\bar{x}, \delta)$,*

$$r(x_{k+1}) \leq qr(x_k) + C_2 r(x_k)^2.$$

Proof. Write $r_k := r(x_k) = d_M(x_k)$, $y_k := P_M(x_k)$, $N_k := N_{y_k}M$, and set $p_k := P_E(y_k)$. Since $E = \bar{x} + L$ is affine, we have $p_k - y_k \in L^\perp$, $x_{k+1} - p_k \in L$.

By (4.2), after shrinking the neighborhood of \bar{x} if necessary, there exists $G > 0$ such that

$$(4.9) \quad r(x_{k+1}) \leq \|P_{N_k}(x_{k+1} - y_k)\| + G\|x_{k+1} - y_k\|^2.$$

Now x_{k+1} minimizes

$$x \mapsto \frac{1}{2}\|x - y_k\|^2 + \frac{1}{2\mu_k}\|P_{N_k}(x - y_k)\|^2 \quad \text{over } E = p_k + L,$$

so the first-order optimality condition is obtained by requiring the gradient to be orthogonal to the feasible direction space L , namely

$$P_L \left[(x_{k+1} - y_k) + \frac{1}{\mu_k} P_{N_k}(x_{k+1} - y_k) \right] = 0.$$

Using $P_L(p_k - y_k) = 0$, this gives $x_{k+1} - y_k = (p_k - y_k) - \frac{1}{\mu_k} P_L P_{N_k}(x_{k+1} - y_k)$. Applying P_{N_k} to this identity and rearranging terms, we obtain

$$(4.10) \quad \left(I + \frac{1}{\mu_k} P_{N_k} P_L \right) P_{N_k}(x_{k+1} - y_k) = P_{N_k}(p_k - y_k).$$

Consider the operator

$$(4.11) \quad B_k := I + \frac{1}{\mu_k} P_{N_k} P_L : N_k \rightarrow N_k.$$

For any $n \in N_k$, $\langle B_k n, n \rangle = \|n\|^2 + \frac{1}{\mu_k} \|P_L n\|^2 \geq \|n\|^2$. Hence B_k is invertible and $\|B_k^{-1}\| \leq 1$. Therefore, from (4.10),

$$(4.12) \quad \|P_{N_k}(x_{k+1} - y_k)\| \leq \|P_{N_k}(p_k - y_k)\|.$$

Next, by (4.3), there exists $G' > 0$ such that

$$(4.13) \quad \|P_{N_k}(p_k - y_k)\| \leq d_M(p_k) + G'\|p_k - y_k\|^2.$$

Since $p_k = P_E(y_k)$ and $x_k \in E$,

$$(4.14) \quad \|p_k - y_k\| = d_E(y_k) \leq \|x_k - y_k\| = r_k.$$

Moreover, $p_k = P_E(P_M(x_k))$ is one alternating-projection step from $x_k \in E$. By the one-step decrease estimate underlying [14, Theorem 6.1], intrinsic transversality implies that, after shrinking the neighborhood if necessary, there exists $q \in (0, 1)$ such that

$$(4.15) \quad d_M(p_k) \leq q d_M(x_k) = q r_k.$$

Combining (4.13)-(4.15), we obtain

$$(4.16) \quad \|P_{N_k}(p_k - y_k)\| \leq q r_k + G' r_k^2.$$

Hence, by (4.12),

$$(4.17) \quad \|P_{N_k}(x_{k+1} - y_k)\| \leq q r_k + G' r_k^2.$$

Substituting (4.17) into (4.9) and using (4.8), we arrive at $r(x_{k+1}) \leq q r_k + G' r_k^2 + 2CGr_k^2 \leq q r(x_k) + C_2 r(x_k)^2$ for some $C_2 > 0$. This completes the proof. \square

In the above proof, we introduced the operator $B_k = I + \frac{1}{\mu_k} P_{N_k} P_L : N_k \rightarrow N_k$ in (4.11), and established the bound $\|B_k^{-1}\| \leq 1$. We emphasize that a sharper estimate requires a uniform lower bound on the action of P_L on N_k . More precisely, under transversality one has, after shrinking the neighborhood if necessary, there exists $\eta > 0$ such that $\|P_L n\| \geq \eta \|n\|$ for all $n \in N_k$. Equivalently, $P_{N_k} P_L|_{N_k}$ is uniformly positive definite on N_k . We will use this stronger estimate in Theorem 4.12.

The following result is a direct corollary of the previous lemma.

COROLLARY 4.6. *Suppose that Assumptions 2.1 and 2.7 hold. There exist constants $\tau \in (0, 1)$ and $C_r > 0$ such that, for any initial point $x_0 \in E$ sufficiently close to \bar{x} , the sequence $\{x_k\}$ generated by Algorithm RN-SLRA satisfies*

$$r(x_k) \leq C_r \tau^k, \quad k = 0, 1, 2, \dots$$

In particular, $\{r(x_k)\}$ converges Q -linearly to 0.

Proof. By Lemma 4.5, there exist $q \in (0, 1)$, $C_2 > 0$ and $\delta > 0$ such that, for $x_k \in E \cap B(\bar{x}, \delta)$,

$$(4.18) \quad r(x_{k+1}) \leq q r(x_k) + C_2 r(x_k)^2.$$

Choose $\varepsilon > 0$ with $\tau := q + C_2 \varepsilon < 1$, and shrink δ so that $r(x) \leq \varepsilon$ on $E \cap B(\bar{x}, \delta)$. By Lemma 4.4, after shrinking δ further, we have $\|x_{k+1} - x_k\| \leq C_1 r(x_k)$ whenever $x_k \in E \cap B(\bar{x}, \delta)$. Take $x_0 \in E$ so close to \bar{x} that $\|x_0 - \bar{x}\| + \frac{C_1}{1-\tau} r(x_0) < \delta$. We prove by induction that $x_k \in B(\bar{x}, \delta)$ and $r(x_k) \leq \tau^k r(x_0)$. Indeed, if this holds up to k , then $r(x_k) \leq \varepsilon$, so (4.18) gives

$$r(x_{k+1}) \leq (q + C_2 r(x_k)) r(x_k) \leq \tau r(x_k) \leq \tau^{k+1} r(x_0),$$

and

$$\|x_{k+1} - \bar{x}\| \leq \|x_0 - \bar{x}\| + C_1 \sum_{j=0}^k r(x_j) \leq \|x_0 - \bar{x}\| + \frac{C_1}{1-\tau} r(x_0) < \delta.$$

Thus $r(x_k) \leq r(x_0)\tau^k$ for all k . Thus $r(x_k) \leq r(x_0)\tau^k \leq C_r\tau^k$, after possibly shrinking the initial neighborhood so that $r(x_0) \leq C_r$. \square

THEOREM 4.7. *Suppose that Assumptions 2.1 and 2.7 hold. For every initial point $x_0 \in E$ sufficiently close to \bar{x} , the sequence $\{x_k\}$ generated by Algorithm RN-SLRA converges to some point $x_\infty \in X$. Moreover, there exist constants $C_X, C_s, C_\infty > 0$ and $\tau \in (0, 1)$ such that*

$$(4.19) \quad d_X(x_k) \leq C_X\tau^k, \quad \|x_{k+1} - x_k\| \leq C_s\tau^k, \quad \|x_k - x_\infty\| \leq C_\infty\tau^k$$

for all $k = 0, 1, 2, \dots$

Proof. By Corollary 4.6, there exist $\tau \in (0, 1)$ and $C_r > 0$ such that $r(x_k) \leq C_r\tau^k$ for all $k = 0, 1, 2, \dots$. On the other hand, by Lemma 4.2, after possibly shrinking the neighborhood of \bar{x} , there exists $\kappa' > 0$ such that $d_X(x) \leq \kappa'r(x)$ for all $x \in E$ in this neighborhood. Hence $d_X(x_k) \leq \kappa'C_r\tau^k$, and the first estimate in (4.19) holds with $C_X := \kappa'C_r$.

Next, by Lemma 4.4, there exists $C_1 > 0$ such that $\|x_{k+1} - x_k\| \leq C_1r(x_k)$. Therefore $\|x_{k+1} - x_k\| \leq C_1C_r\tau^k$, which proves the second estimate in (4.19) with $C_s := C_1C_r$.

Since $\tau \in (0, 1)$, it follows that $\sum_{k=0}^{\infty} \|x_{k+1} - x_k\| < \infty$. Thus $\{x_k\}$ is a Cauchy sequence in E , and hence converges to some $x_\infty \in E$. Moreover, $d_X(x_\infty) \leq d_X(x_k) + \|x_k - x_\infty\| \rightarrow 0$, where the convergence follows from the first estimate in (4.19). Hence $x_\infty \in X$ because X is closed.

Finally, for every k ,

$$(4.20) \quad \|x_k - x_\infty\| \leq \sum_{j=k}^{\infty} \|x_{j+1} - x_j\| \leq C_1C_r \sum_{j=k}^{\infty} \tau^j = \frac{C_1C_r}{1-\tau} \tau^k.$$

Thus the third estimate in (4.19) holds with $C_\infty := \frac{C_1C_r}{1-\tau}$. \square

COROLLARY 4.8. *Suppose that Assumptions 2.1 and 2.7 hold. For every initial point $x_0 \in E$ sufficiently close to \bar{x} , the sequences $\{d_X(x_k)\}$, $\{\|x_{k+1} - x_k\|\}$, and $\{\|x_k - x_\infty\|\}$ all converge R -linearly to 0.*

Proof. This follows immediately from the estimates in (4.19). \square

The next result shows that the limit point selected by Algorithm RN-SLRA has the same order of accuracy as the metric projection onto X . After shrinking the neighborhood if necessary, X is a C^2 embedded submanifold and the local projection P_X is single-valued.

THEOREM 4.9. *Suppose that Assumptions 2.1 and 2.7 hold. There exists a constant $\gamma > 0$ such that, for all initial points $x_0 \in E$ sufficiently close to \bar{x} , the RN-SLRA limit $x_\infty(x_0)$ satisfies*

$$(4.21) \quad \|x_\infty(x_0) - P_X(x_0)\| \leq \gamma\|x_0 - P_X(x_0)\|$$

Proof. Let $p := P_X(x_0)$. By Corollary 4.6, there exist constants $\tau \in (0, 1)$ such that $r(x_k) \leq \tau^k r(x_0)$ for all $k \geq 0$. Moreover, Lemma 4.4 gives $\|x_{k+1} - x_k\| \leq C_1 r(x_k)$ for all $k \geq 0$. Since $p \in X \subset M$, we have $r(x_0) = d_M(x_0) \leq \|x_0 - p\|$. Therefore,

$$(4.22) \quad \begin{aligned} \|x_\infty(x_0) - p\| &\leq \|x_0 - p\| + \sum_{k=0}^{\infty} \|x_{k+1} - x_k\| \leq \|x_0 - p\| + C_1 \sum_{k=0}^{\infty} r(x_k) \\ &\leq \|x_0 - p\| + C_1 \sum_{k=0}^{\infty} \tau^k r(x_0) \leq \left(1 + \frac{C_1}{1 - \tau}\right) \|x_0 - p\|. \end{aligned}$$

This proves (4.21). \square

Before the next remark, we recall that intrinsic transversality is equivalent to clean intersection for intersections of C^2 embedded submanifolds [45]. Therefore, in the present manifold–affine setting, Theorem 4.9 can be interpreted within the clean intersection framework.

Remark 4.10 (First-order retraction-like interpretation under clean intersection).

Assume that E intersects M cleanly at \bar{x} . Since M is of class C^2 and E is an affine subspace, the set X is a C^2 embedded submanifold and satisfies $T_x X = T_x M \cap L$ for all $x \in X$ sufficiently close to \bar{x} . In this case, following [10], the algorithmic limit map can be interpreted as a retraction-like map. More precisely, for $x \in X$ close to \bar{x} and $\xi \in T_x X$ sufficiently small, define $R_x(\xi) := x_\infty(x + \xi)$. Recall that a retraction on a manifold X is a C^1 mapping $R : TX \rightarrow X$ satisfying

$$R_x(0_x) = x, \quad DR_x(0_x) = \text{id}_{T_x X};$$

see, e.g., [2, Definition 4.1.1] or [6, Section 3.4].

Since $\xi \in T_x X$ and X is C^2 , the metric projection onto X satisfies

$$P_X(x + \xi) = x + \xi + O(\|\xi\|^2), \quad \text{dist}(x + \xi, X) = O(\|\xi\|^2).$$

Moreover, Theorem 4.9 gives

$$\|R_x(\xi) - P_X(x + \xi)\| = \|x_\infty(x + \xi) - P_X(x + \xi)\| \leq \gamma \text{dist}(x + \xi, X) = O(\|\xi\|^2).$$

Consequently, $R_x(\xi) = x + \xi + O(\|\xi\|^2)$, which gives a first-order retraction-like expansion. In the special case $\rho = 0$, i.e., $\mu_k \equiv c > 0$, the limiting map can be strengthened to a genuine retraction, and even to a second-order retraction under one additional order of smoothness in Appendix.

4.2. Higher-order Convergence of RN-SLRA under Transversality. We have proved that RN-SLRA converges linearly to a point in X under the assumption that E intersects M intrinsically transversally at $\bar{x} \in X$. If we strengthen the intersection condition to transversality, we obtain sharper local estimates for RN-SLRA. These estimates give a linear-type bound when $\rho = 0$, superlinear convergence when $0 < \rho < 1$, and quadratic convergence when $\rho = 1$. Since transversality implies intrinsic transversality, the lemmas we have proved before still hold.

LEMMA 4.11. *Assume that E and M intersect transversally at \bar{x} . Then, after possibly shrinking the neighborhood of \bar{x} , for all $x_k \in E \cap B_\delta(\bar{x})$, the operator B_k defined in (4.11) is invertible and satisfies*

$$(4.23) \quad \|B_k^{-1}\| \leq \frac{1}{1 + \eta^2/\mu_k} \leq \frac{\mu_k}{\eta^2}.$$

Proof. For any $n \in N_k$, using Lemma 2.3,

$$(4.24) \quad \langle B_k n, n \rangle = \|n\|^2 + \frac{1}{\mu_k} \|P_L n\|^2 \geq \left(1 + \frac{\eta^2}{\mu_k}\right) \|n\|^2.$$

Hence B_k is invertible and (4.23) holds. \square

THEOREM 4.12 (Convergence under transversality). *Assume that E and M intersect transversally at \bar{x} . After possibly shrinking the neighborhood of \bar{x} , there exist constants $\delta > 0$, $C_3 > 0$, and $C_4 > 0$ such that, for all $x_k \in E \cap B(\bar{x}, \delta)$,*

$$(4.25) \quad r(x_{k+1}) \leq C_3 r(x_k)^{1+\rho}, \quad d_X(x_{k+1}) \leq C_4 d_X(x_k)^{1+\rho}.$$

In particular, the residual sequence $\{r(x_k)\}$ and the distance sequence $\{d_X(x_k)\}$ converge to 0 with Q -order at least $1 + \rho$.

Proof. We keep the notation from Lemma 4.5: $r_k := r(x_k) = d_M(x_k)$, $y_k := P_M(x_k)$, $p_k := P_E(y_k)$, and $N_k := N_{y_k} M$. By (4.2), it holds that

$$(4.26) \quad r(x_{k+1}) \leq \|P_{N_k}(x_{k+1} - y_k)\| + G \|x_{k+1} - y_k\|^2$$

for some $G > 0$.

Moreover, from the optimality condition, we already obtained

$$(4.27) \quad \left(I + \frac{1}{\mu_k} P_{N_k} P_L\right) P_{N_k}(x_{k+1} - y_k) = P_{N_k}(p_k - y_k).$$

Define $B_k := I + \frac{1}{\mu_k} P_{N_k} P_L : N_k \rightarrow N_k$. By Lemma 4.11, B_k is invertible and $\|B_k^{-1}\| \leq \frac{\mu_k}{\eta^2}$. Applying this to (4.27), we have

$$(4.28) \quad \|P_{N_k}(x_{k+1} - y_k)\| \leq \frac{\mu_k}{\eta^2} \|P_{N_k}(p_k - y_k)\|.$$

Here we make a more precise estimate of $\|B_k^{-1}\|$ compared to $\|B_k^{-1}\| \leq 1$ of (4.12). This sharper estimate is the key to the higher-order convergence bound.

Since transversality implies intrinsic transversality, applying the same derivation in Lemma 4.5, we obtain

$$(4.29) \quad \|P_{N_k}(p_k - y_k)\| \leq q r_k + G' r_k^2$$

for some $0 < q < 1$ and $G' > 0$. Since $\mu_k = c r_k^\rho$, substituting (4.29) into (4.28) gives

$$(4.30) \quad \|P_{N_k}(x_{k+1} - y_k)\| \leq \frac{c q}{\eta^2} r_k^{1+\rho} + \frac{c G'}{\eta^2} r_k^{2+\rho}.$$

Substituting (4.8) and (4.30) into (4.26), we get

$$(4.31) \quad r(x_{k+1}) \leq \frac{c q}{\eta^2} r_k^{1+\rho} + 2 C G r_k^2 + \frac{c G'}{\eta^2} r_k^{2+\rho}.$$

Since $0 \leq \rho \leq 1$, we have $2 \geq 1 + \rho$, and therefore, after shrinking the neighborhood so that $r_k \leq 1$, $r_k^2 \leq r_k^{1+\rho}$. Thus (4.31) yields

$$(4.32) \quad r(x_{k+1}) \leq C_3 r(x_k)^{1+\rho}$$

for some constant $C_3 > 0$, proving the first estimate in (4.25).

Finally, by Lemma 4.2, $d_X(x_{k+1}) \leq \kappa' r(x_{k+1})$, while trivially $r(x_k) \leq d_X(x_k)$ since $X \subset M$. Hence, using (4.32),

$$(4.33) \quad d_X(x_{k+1}) \leq \kappa' C_3 r(x_k)^{1+\rho} \leq \kappa' C_3 d_X(x_k)^{1+\rho}.$$

This proves the second estimate in (4.25). \square

COROLLARY 4.13 (Quadratic convergence for $\rho = 1$). *Under the assumptions of Theorem 4.12, if $\mu_k = cr(x_k)$, that is, $\rho = 1$, then there exist constants $\delta > 0$, $\widehat{C}_3 > 0$, and $\widehat{C}_4 > 0$ such that, for all $x_k \in E \cap B(\bar{x}, \delta)$,*

$$r(x_{k+1}) \leq \widehat{C}_3 r(x_k)^2, \quad d_X(x_{k+1}) \leq \widehat{C}_4 d_X(x_k)^2.$$

In particular, both $\{r(x_k)\}$ and $\{d_X(x_k)\}$ converge quadratically to 0.

Proof. This is exactly Theorem 4.12 with $\rho = 1$. \square

THEOREM 4.14 (Superlinear convergence of the iterates under transversality). *Assume the setting of Theorem 4.12, with $0 < \rho \leq 1$, and let $x_\infty \in X$ be the limit of the sequence $\{x_k\}$ generated by Algorithm RN-SLRA. Then, after possibly shrinking the neighborhood of \bar{x} , there exist constants $C_5 > 0$ and $C_6 > 0$ such that*

$$(4.34) \quad \|x_{k+1} - x_\infty\| \leq C_5 r(x_k)^{1+\rho}, \quad \|x_{k+1} - x_\infty\| \leq C_6 \|x_k - x_\infty\|^{1+\rho},$$

for all k sufficiently large. In particular, the sequence $\{x_k\}$ converges to x_∞ with Q -order at least $1 + \rho$.

Proof. By Theorem 4.12, there exists $C_3 > 0$ such that

$$(4.35) \quad r(x_{k+1}) \leq C_3 r(x_k)^{1+\rho}.$$

Since $\rho > 0$ and $r(x_k) \rightarrow 0$, after shrinking the neighborhood if necessary, we may assume that $C_3 r(x_k)^\rho \leq \frac{1}{2}$ for all k sufficiently large. Then (4.35) implies $r(x_{k+1}) \leq \frac{1}{2} r(x_k)$, and hence, for every $j \geq k + 1$, $r(x_j) \leq 2^{-(j-k-1)} r(x_{k+1})$.

On the other hand, by Lemma 4.4, $\|x_{j+1} - x_j\| \leq C_1 r(x_j)$. Therefore,

$$(4.36) \quad \|x_{k+1} - x_\infty\| \leq \sum_{j=k+1}^{\infty} \|x_{j+1} - x_j\| \leq C_1 \sum_{j=k+1}^{\infty} r(x_j) \leq 2C_1 r(x_{k+1}).$$

Combining (4.35) and (4.36), one has

$$(4.37) \quad \|x_{k+1} - x_\infty\| \leq 2C_1 C_3 r(x_k)^{1+\rho},$$

which proves the first estimate in (4.34) with $C_5 := 2C_1 C_3$.

Finally, since $x_\infty \in X \subset M$, $r(x_k) = d_M(x_k) \leq \|x_k - x_\infty\|$. Substituting this into (4.37), we get

$$(4.38) \quad \|x_{k+1} - x_\infty\| \leq 2C_1 C_3 \|x_k - x_\infty\|^{1+\rho},$$

which proves the second estimate in (4.34) with $C_6 := 2C_1 C_3$. \square

COROLLARY 4.15 (Quadratic convergence of the iterates for $\rho = 1$). *Under the assumptions of Theorem 4.14, if $\rho = 1$, then there exists a constant $C_7 > 0$ such that*

$$(4.39) \quad \|x_{k+1} - x_\infty\| \leq C_7 \|x_k - x_\infty\|^2$$

for all k sufficiently large. In particular, $\{x_k\}$ converges quadratically to x_∞ .

Proof. This is exactly the second estimate in (4.34) with $\rho = 1$. \square

4.3. Convergence Analysis of iRN-SLRA. In this subsection, we show that iRN-SLRA still enjoys local linear convergence under the intrinsic transversality condition. Under the transversality condition, it also retains the local superlinear and quadratic convergence properties.

We use the following notation throughout. Let

$$\tilde{r}_k := \|x_k - y_k\|, \quad \mu_k := c\tilde{r}_k^\rho, \quad c > 0, \quad \rho \in [0, 1].$$

We also keep the notation $r_k := d_M(x_k)$. Furthermore, we denote by $p_k := P_E(y_k)$ the projection of y_k onto E .

We begin by relating the exact residual r_k and the inexact residual \tilde{r}_k .

LEMMA 4.16. *Suppose that $y_k \in M$ satisfies $\|x_k - y_k\| \leq \sigma d_M(x_k)$, $\sigma \geq 1$. Then $r_k \leq \tilde{r}_k \leq \sigma r_k$. Consequently, we have*

$$c r_k^\rho \leq \mu_k = c \tilde{r}_k^\rho \leq c \sigma^\rho r_k^\rho.$$

Proof. Since $r_k = d_M(x_k)$ and $y_k \in M$, we have $r_k \leq \|x_k - y_k\| = \tilde{r}_k$. The upper bound follows from the σ -quasioptimality condition. The estimate for μ_k is immediate. \square

The next estimate is the inexact analogue of the step-size bound proved earlier for RN-SLRA. Its proof is identical, once r_k is replaced by \tilde{r}_k .

LEMMA 4.17 (Step-size estimate for iRN-SLRA). *Suppose that Assumptions 2.1 and 2.7 hold. Then there exist $\delta > 0$ and $C_8 > 0$ such that, for all iterates $x_k \in E \cap B(\bar{x}, \delta)$,*

$$\|x_{k+1} - y_k\| \leq C_8 \tilde{r}_k, \quad \|x_{k+1} - x_k\| \leq (C_8 + 1) \tilde{r}_k.$$

Proof. The proof is the same as that of Lemma 4.4. Since $x_k \in E$ and $y_k \in M$, we have

$$(4.40) \quad d_E(y_k) \leq \|x_k - y_k\| = \tilde{r}_k.$$

By Lemma 4.1, we may choose $z_k \in P_X(y_k)$ such that $\|z_k - y_k\| \leq \kappa \tilde{r}_k$. Using z_k as a comparison point in the local model and invoking the C^2 -geometry of M , we obtain $\Phi_k(z_k) \leq C\tilde{r}_k^2 + C\mu_k^{-1}\tilde{r}_k^4$. Since $\mu_k = c\tilde{r}_k^\rho$ and $\rho \in [0, 1]$, the second term is $O(\tilde{r}_k^{4-\rho}) = O(\tilde{r}_k^2)$. Hence $\Phi_k(z_k) \leq C\tilde{r}_k^2$, and the rest of the argument is identical to the proof of Lemma 4.4. \square

We now prove local linear convergence under intrinsic transversality. The argument reuses the residual-contraction proof for RN-SLRA, with the alternating-projection comparison point $p_k = P_E(y_k)$.

THEOREM 4.18 (Local linear convergence under intrinsic transversality). *Suppose that Assumptions 2.1 and 2.7 hold. Let $q \in (0, 1)$ be the local one-step alternating-projection decrease constant in the order $M \rightarrow E \rightarrow M$, which follows from the equivalence between intrinsic transversality and separability in Lemma 2.8. Suppose that the quasioptimality constant σ is chosen such that $q_\sigma := \sigma q < 1$. Then the iRN-SLRA iterates satisfy*

$$r_{k+1} \leq q_\sigma r_k + C r_k^2$$

for all k sufficiently large. Consequently, for every $x_0 \in E$ sufficiently close to \bar{x} , there exists $x_\infty \in X$ such that $x_k \rightarrow x_\infty$ locally linearly.

Proof. By Lemma 2.8, Assumption 2.7 implies separability in the order $M \rightarrow E \rightarrow M$. Hence, after shrinking the neighborhood if necessary, there exists $q \in (0, 1)$ such that

$$d_M(P_E(y)) \leq qd_E(y)$$

for all $y \in M$ sufficiently close to \bar{x} . Applying this estimate to y_k , and using $p_k = P_E(y_k)$, $x_k \in E$, and $\|x_k - y_k\| \leq \sigma r_k$, we obtain

$$d_M(p_k) \leq qd_E(y_k) \leq q\|y_k - x_k\| \leq q\sigma r_k.$$

The optimality condition for x_{k+1} remains unchanged. By (4.13)

$$\|P_{N_{y_k}M}(p_k - y_k)\| \leq d_M(p_k) + G'\|p_k - y_k\|^2.$$

Since $p_k = P_E(y_k)$ and $x_k \in E$, by (4.40), we have $\|p_k - y_k\| \leq \tilde{r}_k$. Therefore, $\|P_{N_{y_k}M}(x_{k+1} - y_k)\| \leq q\sigma r_k + G'\tilde{r}_k^2$. Combining this with Lemma 4.17 and Lemma 4.16, we obtain $r_{k+1} \leq q\sigma r_k + C\tilde{r}_k^2$.

Shrinking the neighborhood so that $q\sigma + Cr_k \leq \theta < 1$, we get $r_k \leq \theta^k r_0$. Moreover, by Lemmas 4.17 and 4.16, $\|x_{k+1} - x_k\| \leq C'r_k$. Hence $\sum_k \|x_{k+1} - x_k\| < \infty$, so $x_k \rightarrow x_\infty$. Since $x_k \in E$ and $r_k = d_M(x_k) \rightarrow 0$, we have $x_\infty \in X$. Finally,

$$\|x_k - x_\infty\| \leq C' \sum_{j=k}^{\infty} r_j \leq \frac{C'}{1-\theta} \theta^k r_0,$$

which proves local linear convergence. \square

Remark 4.19 (Quasioptimal alternating projections as a limiting case). If the regularization parameter is formally set to $\mu_k = \infty$, the iRN-SLRA step reduces to

$$x_{k+1} = P_E(y_k), \quad y_k \in M, \quad \|x_k - y_k\| \leq \sigma d_M(x_k),$$

which is a quasioptimal alternating-projection step. Therefore, Theorem 4.18 also yields local linear convergence of quasioptimal alternating projections in the manifold–affine setting under intrinsic transversality, provided $q\sigma < 1$. This complements existing quasioptimal alternating-projection results of [7], by covering the clean-intersection manifold–affine setting. \blacksquare

Under transversality, the proof simplifies further: the comparison point p_k still enters only through first-order information, while the regularized Newton correction suppresses the normal component by an additional factor μ_k . This yields the same high-order estimate as in the exact-projection case.

THEOREM 4.20 (Higher-order convergence under transversality). *Suppose that Assumption 2.1 holds and that E and M intersect transversally at \bar{x} . Let $\mu_k = c\tilde{r}_k^\rho$ with $c > 0$ and $\rho \in (0, 1]$. Then, for all iterates sufficiently close to \bar{x} ,*

$$r_{k+1} \leq C_9 r_k^{1+\rho} + C_{10} r_k^2.$$

Consequently:

- if $0 < \rho < 1$, then the method converges superlinearly with order $1 + \rho$;
- if $\rho = 1$, then the method converges quadratically.

Proof. By the optimality condition for the second step,

$$\left(I + \frac{1}{\mu_k} P_{N_{y_k}M} P_L\right) P_{N_{y_k}M}(x_{k+1} - y_k) = P_{N_{y_k}M}(p_k - y_k).$$

Let $B_k := I + \frac{1}{\mu_k} P_{N_{y_k} M} P_L : N_{y_k} M \rightarrow N_{y_k} M$. By Lemma 4.11, there exists $\eta > 0$ such that $\|B_k^{-1}\| \leq \frac{\mu_k}{\eta^2}$. Hence

$$\|P_{N_{y_k} M}(x_{k+1} - y_k)\| \leq \frac{\mu_k}{\eta^2} \|p_k - y_k\| \leq \frac{c}{\eta^2} \tilde{r}_k^{1+\rho},$$

where the last inequality follows from (4.40). By Lemma 4.17, $\|x_{k+1} - y_k\|^2 \leq C\tilde{r}_k^2$. Hence, by (4.9), $r_{k+1} \leq \frac{c}{\eta^2} \tilde{r}_k^{1+\rho} + C\tilde{r}_k^2$. Using Lemma 4.16 gives $r_{k+1} \leq C_9 r_k^{1+\rho} + C_{10} r_k^2$. The stated convergence orders follow immediately. \square

THEOREM 4.21. *Assume that the conditions of Theorem 4.18 hold. Then there exists a constant $\gamma^i > 0$ such that, for all initial points $x_0 \in E$ sufficiently close to \bar{x} , the iRN-SLRA limit $x_\infty^i(x_0)$ satisfies*

$$(4.41) \quad \|x_\infty^i(x_0) - P_X(x_0)\| \leq \gamma^i \|x_0 - P_X(x_0)\|.$$

Proof. Let $p := P_X(x_0)$. By Lemma 4.16, $\tilde{r}_k \leq \sigma r_k$, while Theorem 4.18 gives $r_k \leq C\tau^k r_0$ for some $\tau \in (0, 1)$. Moreover, Lemma 4.17 gives $\|x_{k+1} - x_k\| \leq (C_8 + 1)\tilde{r}_k$. Since $p \in X \subset M$, we have $r_0 = d_M(x_0) \leq \|x_0 - p\|$. Arguing as in (4.22), we obtain (4.41). \square

Remark 4.22 (Retraction interpretation for iRN-SLRA under clean intersection).

Assume that the clean intersection setting in Remark 4.10 holds. For $x \in X$ close to \bar{x} and $\xi \in T_x X$ sufficiently small, define

$$R_x^i(\xi) := x_\infty^i(x + \xi).$$

Since X is a C^2 embedded submanifold, $P_X(x + \xi) = x + \xi + O(\|\xi\|^2)$ and $\text{dist}(x + \xi, X) = O(\|\xi\|^2)$. By Theorem 4.21, $\|R_x^i(\xi) - P_X(x + \xi)\| = O(\|\xi\|^2)$. Hence $R_x^i(\xi) = x + \xi + O(\|\xi\|^2)$, and R^i has the same first-order retraction interpretation as in Remark 4.10.

5. Experimental Results. In this section, we test our algorithm on some applications of structured low-rank approximation, and compare it with representative existing methods.¹ To demonstrate the ability of our algorithm to handle problems with poor intersection conditions, we will construct some specific examples. Further diagnostics indicating the failure of transversality and supporting intrinsic transversality for these examples are reported in Appendix. All experiments were conducted in Python 3.9.13 on an Ubuntu 22.04 server equipped with dual AMD EPYC 9754 128-core processors (512 logical threads) and 1 TB of RAM.

5.1. Small-scale SLRA Problems. In this section, we construct small-scale SLRA problems that do not satisfy the transversality condition, in order to illustrate the following phenomena:

- RN-SLRA may exhibit either superlinear or only linear local convergence, depending on the geometry;
- In some cases, Newton-SLRA may diverge while RN-SLRA converges;
- Under intrinsic transversality, the theory guarantees only local linear convergence, but RN-SLRA can still converge much faster than Cadzow in ill-conditioned examples.

¹Our Python code is available at <https://github.com/reniusll/Regularized-Newton-SLRA>

All small-scale examples are SLRA problems with artificially constructed affine subspaces and the 4×4 rank-2 manifold \mathcal{D}_2 . They are constructed near $x^* = \text{diag}(4, \sigma_2, 0, 0)$, where $\sigma_2 > 0$ is small. The parameter σ_2 controls the local geometry of the rank constraint: smaller σ_2 leads to a more ill-conditioned low-rank geometry and worsens the conditioning of the tangent-space system [17, 9].

We choose the affine subspace in the form $E = x^* + \text{span}(B_1, B_2, B_3, B_4)$, where the directions B_i are obtained by orthonormalizing prescribed raw directions. These raw directions are chosen mainly in the tangent space $T_{x^*}\mathcal{D}_r$, with a small number of normal components added. Thus each direction can be decomposed as $B_i = T_i + N_i$, where $T_i \in T_{x^*}\mathcal{D}_r$, and $N_i \in N_{x^*}\mathcal{D}_r$.

For the diagonal point $x^* = \text{diag}(4, \sigma_2, 0, 0)$, we use the natural singular-vector coordinates. In these coordinates, the entries coupling the leading and trailing two coordinates give tangent directions, whereas the lower-right 2×2 block gives normal directions. For instance, $E_{13}, E_{31}, E_{24}, E_{42} \in T_{x^*}\mathcal{D}_r$, while $E_{33}, E_{34}, E_{43}, E_{44} \in N_{x^*}\mathcal{D}_r$.

The normal components are chosen to be linearly dependent. Indeed, by the definition of the matrix A in (3.2), for a normal basis element $N_{ab} = u_a v_b^\top$, we have $A_{(a,b),i}(x^*) = \langle N_{ab}, B_i \rangle = u_a^\top B_i v_b = u_a^\top N_i v_b$. Hence $A(x^*)$ depends only on the normal components N_i . If these components are linearly dependent, then $A(x^*)$ is rank deficient. Since transversality at x^* is equivalent to the full-rank condition of $A(x^*)$, the constructed examples violate the transversality condition.

Finally, the initial point is taken as $x_0 = x^* + \sum_{i=1}^4 a_i B_i$, which is a small perturbation of x^* within the affine space E . The explicit choices of the raw directions and coefficients a_i are given in the individual examples below.

5.1.1. Example 1: Newton-SLRA diverges while RN-SLRA converges.

We first take $x^* = \text{diag}(4, 0.02, 0, 0)$, and define directions:

$$\begin{cases} \tilde{B}_1 = E_{13} + 0.7E_{31} + E_{33}, & \tilde{B}_2 = E_{24} - 0.6E_{42} + E_{33}, \\ \tilde{B}_3 = E_{34} + 0.2E_{12}, & \tilde{B}_4 = E_{44} - 0.1E_{21}. \end{cases}$$

The actual basis B_1, \dots, B_4 is obtained from $\tilde{B}_1, \dots, \tilde{B}_4$ by Gram-Schmidt orthonormalization. The initial point is then fixed as $x_0 = x^* + 0.02 \sum_{i=1}^4 a_i B_i$, with $a = (-0.98912135, -0.36778665, 1.28792526, 0.19397442)$.

We compare the numerical performance of Newton-SLRA and Algorithm 3.1 (denoted as RN-SLRA). We set the parameters of RN-SLRA to $c = 3 \times 10^{-7}$ and $\rho = 1$. Our numerical results are presented in Fig. 1.

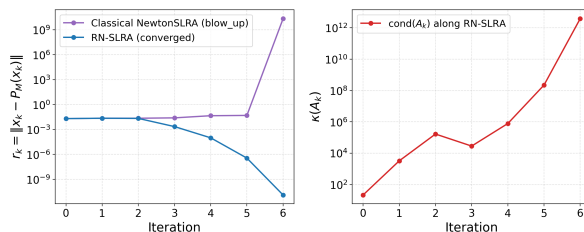


FIG. 1. Comparison of Newton-SLRA and RN-SLRA in Example 1.

RN-SLRA converges in 7 steps, taking 0.001852s, while Newton-SLRA diverges. From the right plot, we can see that the condition number of matrix A becomes extremely large during the iteration process of RN-SLRA, while RN-SLRA still con-

verges rapidly. This example illustrates the stabilizing effect of the regularization term in a nontransversal SLRA problem.

To further check that the above behavior is not caused by a single specially chosen initial point, we also perform a random initialization test on the same example. We generate $x_0 = x^* + \alpha \sum_{i=1}^4 a_i B_i$, where $a = (a_1, \dots, a_4)$ is obtained by sampling a standard Gaussian vector in \mathbb{R}^4 and normalizing it to satisfy $\|a\|_2 = 1$. The radius α is sampled independently from the uniform distribution $\alpha \sim U(0.01, 0.1)$. We use 1000 random initial points. The parameters of RN-SLRA are kept the same as above. The success rates are reported in Table 2.

TABLE 2
Success rates over 1000 random initial points.

Method	Successful runs	Success rate
Newton-SLRA	591/1000	59.1%
RN-SLRA	1000/1000	100%

The result shows that Newton-SLRA is sensitive to the initialization in this non-transversal example, whereas RN-SLRA succeeds for all tested initial points. This supports the observation from Fig. 1 that the regularization stabilizes the Newton iteration near this degenerate intersection.

5.1.2. Example 2: linear convergence of RN-SLRA and comparison with Cadzow. In the previous example, we observed the superlinear convergence of RN-SLRA. We now construct an example for which RN-SLRA exhibits only linear local convergence. This shows that the theoretical linear convergence rate of RN-SLRA is, in general, not improvable. Moreover, using the same example, we compare RN-SLRA with the Cadzow algorithm and show that RN-SLRA can converge much faster, although both algorithms are linearly convergent.

Similar to the previous construction process, we take $x^* = \text{diag}(4, 0.1, 0, 0)$, and

$$\begin{cases} \tilde{B}_1 = E_{13} + 0.6E_{31} + 1.0E_{33}, & \tilde{B}_2 = E_{24} - 0.5E_{42} + 1.0E_{33}, \\ \tilde{B}_3 = E_{34} + 0.1E_{12} + 0.2E_{44}, & \tilde{B}_4 = E_{43} - 0.1E_{21} + 0.6E_{44} + 0.4E_{33}. \end{cases}$$

The initial point is chosen as $x_0 = x^* + 0.01 \sum_{i=1}^4 a_i B_i$, with $a = (1, -1, 0.5, 0.2)$. We set the parameters of RN-SLRA to $c = 0.001$ and $\rho = 1$. On this example, RN-SLRA converges linearly in 10 steps, taking 0.002545s, with an approximate convergence rate $q = 0.2501$.

We further compare the numerical performance of RN-SLRA and Cadzow on the same example with the same parameters. For both algorithms, the maximal number of iterations is set to 1000. The numerical results are presented in Table 3. The residual ratio is the median of the last five values of r_{k+1}/r_k , with $r_k = \|x_k - P_{D_r}(x_k)\|$.

TABLE 3
Comparison of Cadzow and RN-SLRA in Example 2.

Method	Iter.	Time (s)	Final residual	Residual ratio
Cadzow	1000(max)	0.067744	1.03782e-4	0.9993
RN-SLRA	11	0.002545	6.78165e-11	0.2501

The results show that RN-SLRA converges much faster than Cadzow on this example. This behavior is consistent with the local geometry of the problem: alternating projections can be slow when the two sets meet with a very small effective angle, as in the simple case of two nearly parallel intersecting lines. Our constructed example

exhibits a similar local geometry near the intersection point. Thus, this example illustrates that RN-SLRA may have only linear local convergence under nontransversality, but can still be much faster than Cadzow.

5.2. Large-scale SLRA Problems. We construct the intersection point x^* and the affine subspace E in large-scale experiments using a similar method as before, and choose the initial point as $x_0 = P_E(x^* + \alpha G)$, where $G_{ij} \sim N(0, 1)$ are i.i.d. We compare RN-SLRA and Cadzow in nine large-scale experiments; see Fig. 2, where n, m are the matrix dimensions, $p = \dim E$, and r is the target rank. For each tuple (n, m, p, r) , both methods use the same initial point, with $\alpha = 0.05$ for the 100×100 cases, $\alpha = 0.02$ for the larger cases, and stopping tolerance 10^{-8} .

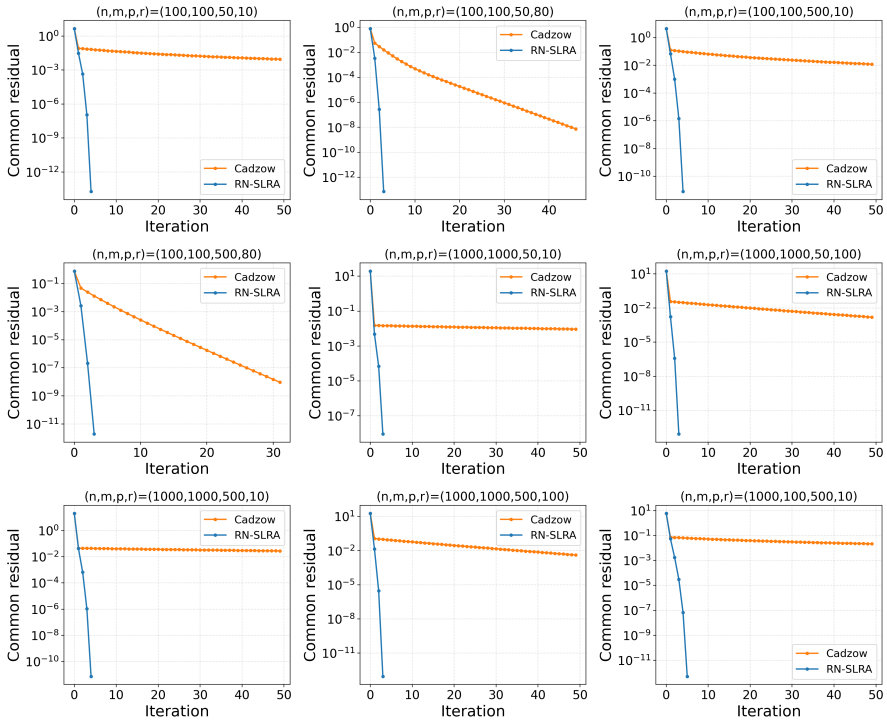


FIG. 2. Large-scale SLRA Problems.

As shown in Fig. 2, RN-SLRA converges within five iterations in all cases, whereas Cadzow converges much more slowly.

5.3. Low-Rank Approximation of Hankel Matrices. We now test the performance of RN-SLRA for low-rank approximation of Hankel matrices [37]. We compare RN-SLRA with four representative baseline families for Hankel structured low-rank approximation: Cadzow; VP-SLRA, based on variable projection and reduced nonlinear optimization for affinely structured SLRA [34]; STLN, which approaches the problem from a structured error-correction perspective [38, 39]; and Gradient-system, based on low-rank factor updates with a Hankel penalty [16].

We will construct a single example and then perform both a noise sweep and an outlier sweep to compare RN-SLRA with the baselines on geometrically degenerate Hankel low-rank approximation problems.

5.3.1. Single example. We consider a 7×5 rank-4 Hankel matrix $H_c = (\nu_{i+j-1})$, where $\nu_i = \sum_{\ell=1}^4 \beta_\ell z_\ell^i$ for $i = 1, \dots, 11$. Here $\beta = (1.2, 0.9, 1.0, 1.1)$ and $z = (e^{-0.2}, e^{-0.2+10^{-3}}, e^{-0.35}, e^{-0.5})$. The closeness of the first two poles makes the instance geometrically degenerate.

The perturbed initial matrix is generated as

$$(5.1) \quad H_0 = H_c + \tau \Delta + \eta E_{\text{out}},$$

where Δ is a random Hankel noise matrix, E_{out} is a Hankel matrix supported on the 9-th anti-diagonal, and in this example we choose $\tau = 3 \times 10^{-3}$, $\eta = 1 \times 10^{-2}$. Δ is a Hankel matrix with generating entries picked independently from $\mathcal{N}(0, 1)$.

We set the parameter of RN-SLRA to $c = 1 \times 10^{-7}$, $\rho = 1$. We terminate an algorithm if it stalls or if its iteration count reaches the maximum number 300. The numerical results are presented in Fig. 3.

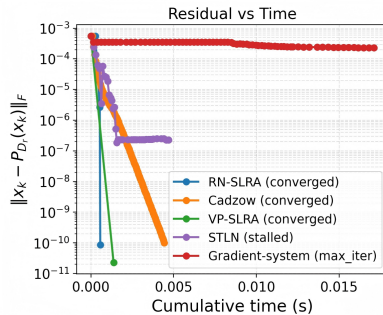


FIG. 3. *Low-Rank Approximation of Hankel Matrices.*

This result shows that RN-SLRA still converges within only a few iterations and rapidly reduces the residual to high accuracy. VP-SLRA also converges to a very small residual, but requires more CPU time than RN-SLRA. Cadzow converges more slowly, while STLN stalls at a moderate residual level, and the gradient-system method fails to make substantial progress within the prescribed maximum number of iterations. These results demonstrate that RN-SLRA remains effective for geometrically degenerate structured low-rank approximation problems, achieving fast convergence and competitive accuracy.

5.3.2. Noise Sweep and Outlier Sweep. We next test the robustness of RN-SLRA under different noise and outlier levels. In both sweeps, the initial point is generated by (5.1), and several independent random Hankel noises Δ are used. For the noise sweep, the outlier level η is fixed and $\tau \in \{10^{-4}, 3 \times 10^{-4}, 10^{-3}, 3 \times 10^{-3}\}$. For the outlier sweep, the noise level τ is fixed and $\eta \in \{0, 10^{-3}, 3 \times 10^{-3}, 10^{-2}\}$. The mean CPU times over 30 random perturbations are reported in Table 4. Here “fail” means that the algorithm does not reach the prescribed tolerance within the iteration limit.

The results show that RN-SLRA remains robust and consistently achieves the smallest mean CPU time across both sweeps. VP-SLRA and Cadzow also converge, but require more time, while STLN and Gradient-system fail on all tested instances. This further illustrates the effectiveness of RN-SLRA on examples with poor geometry.

5.3.3. Large-scale inexact-projection experiment. We finally compare RN-SLRA with iRN-SLRA when the rank- r projection is computed only approximately.

TABLE 4

Mean CPU times with sample standard deviations in seconds for the Hankel noise and outlier sweeps over 30 random perturbations. Here RN, VP, and GS denote RN-SLRA, VP-SLRA, and Gradient-system, respectively.

Sweep	Level	RN	Cadzow	VP	STLN	GS
Noise	10^{-4}	0.0009 ± 0.0003	0.0030 ± 0.0014	0.0028 ± 0.0023	fail	fail
Noise	$3 \cdot 10^{-4}$	0.0009 ± 0.0003	0.0031 ± 0.0014	0.0016 ± 0.0003	fail	fail
Noise	10^{-3}	0.0009 ± 0.0004	0.0034 ± 0.0015	0.0016 ± 0.0004	fail	fail
Noise	$3 \cdot 10^{-3}$	0.0008 ± 0.0002	0.0039 ± 0.0015	0.0016 ± 0.0003	fail	fail
Outlier	0	0.0009 ± 0.0003	0.0035 ± 0.0013	0.0018 ± 0.0005	fail	fail
Outlier	10^{-3}	0.0008 ± 0.0001	0.0039 ± 0.0018	0.0021 ± 0.0013	fail	fail
Outlier	$3 \cdot 10^{-3}$	0.0008 ± 0.0002	0.0032 ± 0.0017	0.0018 ± 0.0002	fail	fail
Outlier	10^{-2}	0.0008 ± 0.0002	0.0036 ± 0.0018	0.0023 ± 0.0009	fail	fail

Here n and m denote the matrix dimensions and r is the target rank. We use larger degenerate Hankel SLRA instances $H_c^{(n,m,3)} \in \mathbb{R}^{n \times m}$ generated from the repeated-pole model $\nu_i = \beta_0 \lambda^i + \beta_1 i \lambda^i + \beta_2 \mu^i$, where the term $i \lambda^i$ induces poor local geometry. We test $(n, m, r) \in \{(120, 160, 3), (200, 280, 3), (350, 500, 3), (700, 1000, 3)\}$.

To keep the instances comparable, the poles are moved closer to one as the matrix size increases and the coefficients are mildly rescaled. For these four sizes, the corresponding $(\lambda, \mu, \beta_0, \beta_1, \beta_2)$ are $(e^{-0.06}, e^{-0.19}, 1.0, 0.09, 0.8)$, $(e^{-0.035}, e^{-0.12}, 1.0, 0.06, 0.65)$, $(e^{-0.022}, e^{-0.075}, 1.0, 0.045, 0.55)$, and $(e^{-0.012}, e^{-0.045}, 1.0, 0.025, 0.45)$.

The initial matrix is $H_0 = H_c + \tau \Delta + \eta E_{\text{out}}$, where Δ is random Hankel noise and E_{out} is a Hankel outlier supported on one anti-diagonal. We normalize the perturbations by $\alpha_c = \|H_c\|/\sqrt{mn}$, and set $\tau = 5 \times 10^{-2} \alpha_c$, $\eta = 10^{-1} \alpha_c$. For both methods, we tune $c \in \{10^{-8}, 3 \times 10^{-8}, 10^{-7}, 3 \times 10^{-7}, 10^{-6}\}$ and $\rho \in \{0, 0.5, 1.0\}$. For iRN-SLRA, the rank- r projection is approximated by randomized SVD [19]. We use $\varepsilon_r \in \{0.1, 0.25\}$ as the relative tolerance in the randomized SVD routine, and $s \in \{1, 2, 3\}$ as the number of subspace iterations. The stopping tolerance is 10^{-7} , and the maximum number of outer iterations is 40.

TABLE 5

Large-scale Hankel experiments: iteration counts, CPU times, and final rank residuals.

(n, m, r)	RN-SLRA			iRN-SLRA		
	Iter.	Time (s)	Final residual	Iter.	Time (s)	Final residual
(120,160,3)	6	0.8515	2.62×10^{-10}	4	0.4793	5.60×10^{-10}
(200,280,3)	7	2.8913	1.63×10^{-10}	4	1.3842	3.82×10^{-10}
(350,500,3)	5	9.3378	1.33×10^{-10}	4	6.8277	3.68×10^{-13}
(700,1000,3)	6	98.1399	2.33×10^{-10}	4	58.0918	5.74×10^{-10}

Table 5 shows that iRN-SLRA preserves the robustness of RN-SLRA while reducing the running time. The gain becomes more pronounced at larger scales; for (700, 1000, 3), the time decreases from 98.14 to 58.09 seconds.

6. Conclusion. We proposed RN-SLRA, a regularized Newton-type method for local manifold-affine intersection problems. The method is well defined under intrinsic transversality, where we proved local linear convergence, and achieves order $1+\rho$ under transversality with $\mu_k = cr_k^\rho$, including quadratic convergence when $\rho = 1$. We also developed an inexact variant, iRN-SLRA, and showed that the same local rates are preserved under a suitable quasioptimal projection condition. Numerical experiments illustrate the robustness of RN-SLRA and the efficiency of iRN-SLRA.

REFERENCES

- [1] P.-A. ABSIL, L. AMODEI, AND G. MEYER, *Two newton methods on the manifold of fixed-rank matrices endowed with riemannian quotient geometries*, Computational Statistics, 29 (2014), pp. 569–590.
- [2] P.-A. ABSIL, R. MAHONY, AND R. SEPULCHRE, *Optimization Algorithms on Matrix Manifolds*, Princeton University Press, Princeton, NJ, 2008.
- [3] P.-A. ABSIL AND J. MALICK, *Projection-like retractions on matrix manifolds*, SIAM Journal on Optimization, 22 (2012), pp. 135–158.
- [4] F. ANDERSSON AND M. CARLSSON, *Alternating projections on nontangential manifolds*, Constructive Approximation, 38 (2013), pp. 489–525.
- [5] H. H. BAUSCHKE AND J. M. BORWEIN, *On the convergence of von neumann’s alternating projection algorithm for two sets*, Set-Valued Analysis, 1 (1993), pp. 185–212.
- [6] N. BOUMAL, *An Introduction to Optimization on Smooth Manifolds*, Cambridge University Press, 2023.
- [7] S. BUDZINSKIY, *Quasioptimal alternating projections and their use in low-rank approximation of matrices and tensors*, Numerische Mathematik, 157 (2025), pp. 1491–1535.
- [8] J. CADZOW, *Signal enhancement—a composite property mapping algorithm*, IEEE Transactions on Acoustics, Speech, and Signal Processing, 36 (1988), pp. 49–62.
- [9] G. CERUTI, C. LUBICH, AND H. WALACH, *Time integration of symmetric and anti-symmetric low-rank matrices and tucker tensors*, BIT Numerical Mathematics, 60 (2020), pp. 591–614.
- [10] S. CHEN, Y. HE, AND W. HUANG, *Retractions by alternating projections*, arXiv:2605.17384, (2026).
- [11] M. T. CHU, R. E. FUNDERLIC, AND R. J. PLEMMONS, *Structured low rank approximation*, Linear Algebra and its Applications, 366 (2003), pp. 157–172.
- [12] F. DEUTSCH, *Best Approximation in Inner Product Spaces*, CMS Books in Mathematics, Springer, New York, 2001.
- [13] D. DRUSVYATSKIY, *Slope and Geometry in Variational Mathematics*, PhD thesis, Cornell University, 2013.
- [14] D. DRUSVYATSKIY, A. D. IOFFE, AND A. S. LEWIS, *Transversality and alternating projections for nonconvex sets*, Foundations of Computational Mathematics, 15 (2015), pp. 1637–1651.
- [15] D. DRUSVYATSKIY AND A. S. LEWIS, *Local linear convergence for inexact alternating projections on nonconvex sets*, Vietnam J. Math., 47 (2019), pp. 669–681.
- [16] A. FAZZI, N. GUGLIELMI, AND I. MARKOVSKY, *A gradient system approach for hankel structured low-rank approximation*, Linear Algebra and its Applications, 623 (2021), pp. 236–257.
- [17] F. FEPPON AND P. F. J. LERMUSIAUX, *A geometric approach to dynamical model-order reduction*, SIAM Journal on Matrix Analysis and Applications, 39 (2018), pp. 510–538.
- [18] J. GILLARD, *Cadzow’s basic algorithm, alternating projections and singular spectrum analysis*, Statistics and Its Interface, 3 (2010), pp. 335–343.
- [19] N. HALKO, P.-G. MARTINSSON, AND J. A. TROPP, *Finding structure with randomness: Probabilistic algorithms for constructing approximate matrix decompositions*, SIAM Review, 53 (2011), pp. 217–288.
- [20] A. D. IOFFE, *Metric regularity—a survey. part 1. theory*, Journal of the Australian Mathematical Society, 101 (2016), pp. 188–243.
- [21] A. D. IOFFE, *Transversality in variational analysis*, Journal of Optimization Theory and Applications, 174 (2017), pp. 343–366.
- [22] P. JAIN, P. NETRAPALLI, AND S. SANGHAVI, *Low-rank matrix completion using alternating minimization*, in Proceedings of the Forty-Fifth Annual ACM Symposium on Theory of Computing, 2013, pp. 665–674.
- [23] E. KALTOFEN, Z. YANG, AND L. ZHI, *Structured low rank approximation of a Sylvester matrix*, in Symbolic-Numeric Computation, Trends in Mathematics, Birkhäuser, 2007, pp. 69–83.
- [24] A. Y. KRUGER, D. R. LUKE, AND N. H. THAO, *About subtransversality of collections of sets*, Set-Valued and Variational Analysis, 25 (2017), pp. 701–729.
- [25] A. Y. KRUGER AND N. H. THAO, *Regularity of collections of sets and convergence of inexact alternating projections*, Journal of Convex Analysis, 23 (2016), pp. 823–847.
- [26] R. M. LARSEN, *Lanczos bidiagonalization with partial reorthogonalization*, Tech. Report DAIMI PB-537, Department of Computer Science, Aarhus University, 1998.
- [27] A. S. LEWIS, D. R. LUKE, AND J. MALICK, *Local linear convergence for alternating and averaged nonconvex projections*, Foundations of Computational Mathematics, 9 (2009), pp. 485–513.
- [28] A. S. LEWIS AND J. MALICK, *Alternating projections on manifolds*, Mathematics of Operations Research, 33 (2008), pp. 216–234.

- [29] D.-H. LI, M. FUKUSHIMA, L. QI, AND N. YAMASHITA, *Regularized newton methods for convex minimization problems with singular solutions*, Computational Optimization and Applications, 28 (2004), pp. 131–147.
- [30] D. R. LUKE, M. TEBoulLE, AND N. H. THAO, *Necessary conditions for linear convergence of iterated expansive, set-valued mappings*, Mathematical Programming, 180 (2020), pp. 1–31.
- [31] I. MARKOVSKY, *Structured low-rank approximation and its applications*, Automatica, 44 (2008), pp. 891–909.
- [32] I. MARKOVSKY, *System identification in the behavioral setting*, in Latent Variable Analysis and Signal Separation, vol. 9237 of Lecture Notes in Computer Science, Springer, 2015, pp. 235–242.
- [33] I. MARKOVSKY AND P. L. DRAGOTTI, *Using hankel structured low-rank approximation for sparse signal recovery*, in Latent Variable Analysis and Signal Separation, vol. 10891 of Lecture Notes in Computer Science, Springer, 2018, pp. 479–487.
- [34] I. MARKOVSKY AND K. USEVICH, *Software for weighted structured low-rank approximation*, Journal of Computational and Applied Mathematics, 256 (2014), pp. 278–292.
- [35] D. NOLL AND A. RONDEPIERRE, *On local convergence of the method of alternating projections*, Foundations of Computational Mathematics, 16 (2016), pp. 425–455.
- [36] G. OTTAVIANI, P.-J. SPAENLEHAUER, AND B. STURMFELS, *Exact solutions in structured low-rank approximation*, SIAM Journal on Matrix Analysis and Applications, 35 (2014), pp. 1521–1542.
- [37] H. PARK, L. ZHANG, AND J. B. ROSEN, *Low rank approximation of a hankel matrix by structured total least norm*, BIT Numerical Mathematics, 39 (1999), pp. 757–779.
- [38] J. B. ROSEN, H. PARK, AND J. GLICK, *Total least norm formulation and solution for structured problems*, SIAM Journal on Matrix Analysis and Applications, 17 (1996), pp. 110–126.
- [39] J. B. ROSEN, H. PARK, AND J. GLICK, *Structured total least norm for nonlinear problems*, SIAM Journal on Matrix Analysis and Applications, 20 (1998), pp. 14–30.
- [40] É. SHOST AND P. SPAENLEHAUER, *A quadratically convergent algorithm for structured low-rank approximation*, Found Comput Math, 16 (2016), pp. 457–492.
- [41] H. A. SCHWARZ, *Ueber einige abbildungsaufgaben*, Journal für die reine und angewandte Mathematik, 70 (1869), pp. 105–120.
- [42] B. VANDEREYCKEN, *Low-rank matrix completion by riemannian optimization*, SIAM Journal on Optimization, 23 (2013), pp. 1214–1236.
- [43] J. VON NEUMANN, *Functional Operators. II. The Geometry of Orthogonal Spaces*, vol. 22 of Annals of Mathematics Studies, Princeton University Press, Princeton, NJ, 1950.
- [44] N. XIAO, S. WANG, T. TANG, AND K.-C. TOH, *A quadratically convergent alternating projection method for nonconvex sets*, arXiv:2511.22916, (2025).
- [45] Y. YANG, B. GAO, AND Y. XIANG YUAN, *Optimization over the intersection of manifolds*, arXiv:2605.22736, (2026).
- [46] G.-X. YUAN, C.-H. HO, AND C.-J. LIN, *An improved glmnet for l1-regularized logistic regression*, Journal of Machine Learning Research, 13 (2011), pp. 33–41.
- [47] M.-C. YUE, Z. ZHOU, AND A. M.-C. SO, *A family of inexact sqa methods for non-smooth convex minimization with provable convergence guarantees based on the luo-tseng error bound property*, Math. Program, 174 (2019), pp. 327–358.

Appendix A. Numerical Diagnostics of Intrinsic Transversality.

This appendix reports numerical diagnostics supporting the intrinsic transversality condition in the examples used in the numerical experiments.

A.1. Numerical Principle. Let E be the affine constraint set and let D_r be the fixed-rank manifold of rank- r matrices. Around a point $x^* \in E \cap D_r$, we sample nearby points $x \in E$ and $y \in D_r$, and define

$$u = \frac{x - y}{\|x - y\|_F}.$$

We then compute the intrinsic transversality proxy

$$\eta(x, y) = \max \left\{ \text{dist} \left(u, N_{D_r}(y) \right), \text{dist} \left(u, N_E(x) \right) \right\}.$$

Since E is affine, $N_E(x)$ is independent of x . A positive lower bound on $\eta(x, y)$ over nearby sampled pairs indicates that the displacement direction cannot be simultaneously close to both normal geometries, which is the separation expected from intrinsic transversality.

For the small synthetic examples, we also report the singular values of the classical tangent-intersection matrix $A(x^*)$. A zero or nearly zero smallest singular value indicates failure of classical transversality, whereas positive sampled values of η support the weaker intrinsic transversality condition used in this paper.

A.2. Example 1: Newton-SLRA versus RN-SLRA. For the first synthetic example, the singular values of the classical tangent-intersection matrix at the solution are

$$\sigma(A(x^*)) = (0.9950, 0.9806, 0.7645, 0).$$

Thus the classical transversality matrix is rank deficient. Nearby random rank-2 points nevertheless yield positive sampled smallest singular values:

sampling scale	min σ_{\min}	median σ_{\min}	max σ_{\min}
10^{-3}	$5.1222 \cdot 10^{-8}$	$2.7545 \cdot 10^{-6}$	$5.0001 \cdot 10^{-5}$
10^{-2}	$1.2180 \cdot 10^{-4}$	$3.3858 \cdot 10^{-3}$	$5.4935 \cdot 10^{-2}$
$5 \cdot 10^{-2}$	$3.3860 \cdot 10^{-5}$	$7.0428 \cdot 10^{-3}$	$1.4893 \cdot 10^{-1}$

The intrinsic transversality proxy was then computed for nearby pairs $x \in E$ and $y \in D_2$:

scale _{x}	scale _{y}	samples	min η	median η
0.01	0.01	200	0.6611	0.9306
0.01	0.02	200	0.8828	0.9787
0.01	0.05	142	0.9683	0.9937
0.02	0.01	200	0.6706	0.8783
0.02	0.02	200	0.7721	0.9510
0.02	0.05	144	0.8753	0.9896
0.05	0.01	200	0.7323	0.9428
0.05	0.02	200	0.7363	0.9105
0.05	0.05	145	0.7489	0.9585

All sampled minima are bounded away from zero.

A.3. Random Initializations for Example 1. The random-initialization experiment uses the same affine-rank geometry as Example 1 and changes only the initial point distribution. The intrinsic transversality diagnostics are therefore the same as those reported above.

A.4. Linear-Convergence Example. For the selected linear-convergence example, the tangent-intersection singular values at x^* are

$$\sigma(A(x^*)) = (0.9968, 0.9951, 0.7604, 9.2694 \cdot 10^{-21}),$$

so classical transversality again fails numerically. The intrinsic proxy was sampled at scale 0.02 with 80 random pairs, giving

$$\min \eta = 0.7482.$$

This positive value supports intrinsic transversality for this example.

A.5. Cadzow versus RN-SLRA on the Linear-Convergence Example. The Cadzow comparison uses the same geometry as the linear-convergence example. Hence the corresponding diagnostics are

$$\sigma(A(x^*)) = (0.9968, 0.9951, 0.7604, 9.2694 \cdot 10^{-21}), \quad \min \eta = 0.7482.$$

A.6. Large-Scale Synthetic SLRA Examples. For the nine large-scale synthetic SLRA examples, we report a rank bound for the classical transversality matrix and the minimum sampled intrinsic proxy. The proxy is computed over 24 local samples with sampling radius 0.01.

(m, n)	p	r	rank bound	$\min \eta$
(100, 100)	50	10	2	0.9998316
(100, 100)	50	80	2	0.9997508
(100, 100)	500	10	2	0.9995969
(100, 100)	500	80	2	0.9995995
(1000, 1000)	50	10	2	0.9999997
(1000, 1000)	50	100	2	0.9999983
(1000, 1000)	500	10	2	0.9999981
(1000, 1000)	500	100	2	0.9999890
(1000, 100)	500	10	2	0.9999526

In all nine cases, the sampled intrinsic proxy is close to one. In contrast, the recorded transversality rank bound is 2, much smaller than the number of affine constraints p . This is consistent with the construction: the examples are rank deficient in the classical tangent-intersection sense, while retaining a strong sampled intrinsic separation.

A.7. Hankel SLRA Experiments. We also computed the intrinsic transversality proxy for the small Hankel experiments. For each case, 200 sampled pairs were used at each radius $\rho \in \{0.01, 0.02, 0.05\}$. The table reports the smallest sampled value of η over these radii, together with the range of median values. The column $\sigma_{\min}(A)$ gives the smallest singular value of the tangent-restriction matrix when it was explicitly formed.

experiment	(m, n)	r	$\sigma_{\min}(A)$	$\min \eta$	median η range
single example	(7, 5)	4	$4.5647 \cdot 10^{-1}$	0.8628	[0.9788, 0.9800]
noise sweep	(7, 5)	4	$4.5575 \cdot 10^{-1}$	0.8234	[0.9783, 0.9788]
noise sweep	(7, 5)	4	$4.5647 \cdot 10^{-1}$	0.8710	[0.9788, 0.9802]
noise sweep	(8, 5)	2	$4.8981 \cdot 10^{-17}$	0.7718	[0.8812, 0.8838]
outlier sweep	(7, 5)	4	$4.5575 \cdot 10^{-1}$	0.8864	[0.9803, 0.9815]
outlier sweep	(7, 5)	4	$4.5647 \cdot 10^{-1}$	0.8391	[0.9778, 0.9799]
outlier sweep	(8, 5)	2	$4.8981 \cdot 10^{-17}$	0.7627	[0.8761, 0.8792]

For all small Hankel cases, the sampled intrinsic proxy remains bounded away from zero. Some cases have a nearly singular tangent-restriction matrix, while their intrinsic proxy remains positive. This is consistent with the pattern observed in the synthetic SLRA examples.

A.8. Large-Scale Hankel Intrinsic Diagnostics. For the large-scale Hankel benchmark used in Table 5, the tangent-restriction matrix was not explicitly formed. The intrinsic proxy was computed directly from sampled normal-cone distances, using 24 sampled pairs at radius 0.01 for each case.

(m, n)	r	samples	$\min \eta$	median η
(160, 120)	3	24	0.9752	0.9786
(280, 200)	3	24	0.9852	0.9879
(500, 350)	3	24	0.9920	0.9927
(1000, 700)	3	24	0.9961	0.9964

All four large-scale Hankel cases have sampled η -values close to one, providing further numerical evidence of intrinsic separation.

Appendix B. Retraction induced by RN-SLRA in the case $\rho = 0$.

In this appendix we justify the retraction interpretation in Remark 4.10 for the special case $\rho = 0$. In this case the residual-dependent rule $\mu_k = cr_k^\rho$ is understood as the fixed choice $\mu_k \equiv c > 0$.

Let $\Phi_c : E \rightarrow E$ denote the one-step RN-SLRA map with $\mu_k \equiv c$. For $z \in E$ close to X , set $y = P_M(z)$, $Q_y := P_{N_y M}$, and define

$$\Phi_c(z) := \arg \min_{u \in E} \left\{ \frac{1}{2} \|u - y\|^2 + \frac{1}{2c} \|Q_y(u - y)\|^2 \right\}.$$

We first show that, under clean intersection and suitable smoothness, the limiting map of Φ_c defines a genuine retraction on X . We then show that one additional order of smoothness yields a second-order retraction.

THEOREM B.1 (Retraction for RN-SLRA when $\rho = 0$). *Assume that E intersects M cleanly at \bar{x} . Assume further that the fixed-regularization one-step map Φ_c is of class C^2 in a neighborhood of X ; for instance, this holds if M is locally C^3 near \bar{x} . Then, for all $z \in E$ sufficiently close to X , the limit*

$$\Psi_c(z) := \lim_{k \rightarrow \infty} \Phi_c^k(z)$$

exists locally and Ψ_c is C^1 . Consequently,

$$R_x^c(\xi) := \Psi_c(x + \xi), \quad x \in X, \quad \xi \in T_x X,$$

defines a C^1 retraction on X .

Proof. For y close to X , write $p = P_E(y)$. Since every point in E can be written as $p + \ell$ with $\ell \in L$, the subproblem defining $\Phi_c(z)$ is equivalent to minimizing over $\ell \in L$. Its first-order optimality condition is

$$\ell + \frac{1}{c}P_L Q_y(p - y + \ell) = 0.$$

Equivalently,

$$(cI_L + A_y)\ell = -P_L Q_y(p - y), \quad A_y := P_L Q_y|_L.$$

Since A_y is self-adjoint positive semidefinite on L and $c > 0$, the operator $cI_L + A_y$ is uniformly invertible. Hence Φ_c is locally well defined and inherits the assumed smoothness.

For $x \in X$, we have $P_M(x) = x$, $P_E(x) = x$, and hence $\Phi_c(x) = x$. Thus X is a fixed-point manifold of Φ_c . We now compute the derivative of Φ_c at $x \in X$. Let $h \in L$. Since $DP_M(x)h = P_{T_x M}h$, differentiating the optimality system at x gives

$$(cI_L + A_x)\ell' = -P_L Q_x(P_L P_{T_x M}h - P_{T_x M}h), \quad A_x := P_L Q_x|_L.$$

Using $P_{T_x M} = I - Q_x$ and $h \in L$, we have $P_L P_{T_x M}h = h - A_x h$. Hence the right-hand side equals $-A_x(I_L - A_x)h$, and therefore

$$\ell' = -(cI_L + A_x)^{-1}A_x(I_L - A_x)h.$$

Since $D\Phi_c(x)h = P_L P_{T_x M}h + \ell'$, we obtain

$$(B.1) \quad D\Phi_c(x)h = (I_L + c^{-1}A_x)^{-1}(I_L - A_x)h.$$

The operator A_x is self-adjoint and positive semidefinite on L , because

$$\langle A_x h, h \rangle = \langle Q_x h, h \rangle = \|Q_x h\|^2.$$

Moreover,

$$\ker A_x = \{h \in L : Q_x h = 0\} = L \cap T_x M = T_x X,$$

where the last equality follows from clean intersection. Let $W_x := L \ominus T_x X$. Since A_x depends continuously on x and $\dim T_x X$ is locally constant under clean intersection, the nonzero eigenvalues of A_x are locally bounded away from zero. Hence, after shrinking the neighborhood if necessary, there exists $\sigma > 0$ such that

$$(B.2) \quad \langle A_x h, h \rangle \geq \sigma \|h\|^2, \quad h \in W_x, \quad x \in X.$$

Thus $D\Phi_c(x)h = h$ for $h \in T_x X$. If $h \in W_x$ is an eigenvector of A_x with eigenvalue $\lambda \in [\sigma, 1]$, then

$$D\Phi_c(x)h = \frac{1 - \lambda}{1 + \lambda/c}h.$$

Consequently, the derivative is the identity along $T_x X$ and is uniformly contractive on W_x . Therefore X is a normally attracting fixed-point manifold of Φ_c .

We next prove the C^1 regularity of the limiting map. We work in a local tubular coordinate system in E around X . Namely, for $z \in E$ close to X , write

$$z = s + w, \quad s = P_X(z), \quad w \in W_s := L \ominus T_s X.$$

Using a smooth local frame of the bundle W_s , we identify the spaces W_s with a fixed Euclidean space. In these coordinates, write

$$\Phi_c(s, w) = (s + a(s, w), B_s w + b(s, w)).$$

Since every point of X is fixed by Φ_c , and since the derivative of Φ_c is the identity in the tangent direction and has no first-order tangential response in the normal direction, we have

$$a(s, 0) = 0, \quad b(s, 0) = 0, \quad D_w a(s, 0) = 0, \quad D_w b(s, 0) = 0.$$

Moreover, by the uniform contraction on W_s , after shrinking the neighborhood if necessary,

$$\|B_s\| \leq q < 1$$

uniformly for $s \in X$ close to \bar{x} . Since Φ_c is C^2 , it follows that

$$(B.3) \quad a(s, w) = O(\|w\|^2), \quad b(s, w) = O(\|w\|^2).$$

Moreover,

$$(B.4) \quad \begin{aligned} D_s a(s, w) &= O(\|w\|), & D_w a(s, w) &= O(\|w\|), \\ D_s b(s, w) &= O(\|w\|), & D_w b(s, w) &= O(\|w\|). \end{aligned}$$

All estimates are local and uniform.

Let

$$(s_{k+1}, w_{k+1}) = \Phi_c(s_k, w_k), \quad (s_0, w_0) = (s, w).$$

The normal component satisfies

$$w_{k+1} = B_{s_k} w_k + b(s_k, w_k).$$

Choose $\theta \in (q, 1)$. By (B.3), after shrinking the neighborhood if necessary, the non-linear term $b(s, w)$ is small enough so that

$$(B.5) \quad \|w_k\| \leq C\theta^k \|w_0\|.$$

Moreover,

$$s_{k+1} - s_k = a(s_k, w_k),$$

and hence, by (B.3) and (B.5),

$$\sum_{k=0}^{\infty} \|s_{k+1} - s_k\| \leq C \sum_{k=0}^{\infty} \|w_k\|^2 \leq C \|w_0\|^2.$$

Therefore s_k converges to a limit s_∞ , $w_k \rightarrow 0$, and

$$(B.6) \quad \Psi_c(s, w) = (s_\infty, 0), \quad s_\infty = s + \sum_{k=0}^{\infty} a(s_k, w_k).$$

It remains to justify the C^1 dependence on the initial point. Differentiating the recursions and using (B.4), (B.5), and the uniform contraction in the w -equation gives, by a standard induction on the differentiated recursions,

$$(B.7) \quad \|D_z w_k\| \leq C\theta^k, \quad \sup_k \|D_z s_k\| \leq C.$$

By the chain rule and (B.4),

$$\begin{aligned} \|D_z a(s_k, w_k)\| &\leq C \|w_k\| (\|D_z s_k\| + \|D_z w_k\|) \\ &\leq C' \theta^k. \end{aligned}$$

Thus the derivative series

$$D_z s_0 + \sum_{k \geq 0} D_z a(s_k, w_k)$$

converges uniformly. It follows from (B.6) that s_∞ is C^1 , and therefore $\Psi_c(s, w) = (s_\infty(s, w), 0)$ is C^1 .

Finally, define, for $x \in X$ close to \bar{x} and $\xi \in T_x X$ sufficiently small,

$$R_x^c(\xi) := \Psi_c(x + \xi).$$

Since Ψ_c is C^1 , $R^c : TX \rightarrow X$ is C^1 . Also, $\Psi_c(x) = x$ for every $x \in X$. Hence, for any $\xi \in T_x X$, taking a C^1 curve $\gamma(t) \subset X$ with $\gamma(0) = x$ and $\gamma'(0) = \xi$, we have $\Psi_c(\gamma(t)) = \gamma(t)$, and therefore $D\Psi_c(x)\xi = \xi$. Consequently,

$$R_x^c(0_x) = x, \quad DR_x^c(0_x) = \text{id}_{T_x X}.$$

Thus R^c is a C^1 retraction on X . \square

THEOREM B.2 (Second-order retraction for RN-SLRA when $\rho = 0$). *Assume the hypotheses of Theorem B.1. Assume in addition that the fixed-regularization one-step map Φ_c is of class C^3 in a neighborhood of X ; for instance, this holds if M is locally C^4 near \bar{x} . Then the limiting map Ψ_c is C^2 . Consequently,*

$$R_x^c(\xi) := \Psi_c(x + \xi), \quad x \in X, \quad \xi \in T_x X,$$

defines a second-order retraction on X .

Proof. We use the notation and local coordinates from the proof of Theorem B.1. Since now Φ_c is C^3 , the functions a and b satisfy the following strengthened local estimates. Indeed, the fixed-point property on X gives $a(s, 0) = b(s, 0) = 0$, and the normal-form construction gives $D_w a(s, 0) = D_w b(s, 0) = 0$. Hence, by Taylor's formula in the normal variable w , uniformly for s near \bar{x} ,

$$a(s, w) = O(\|w\|^2), \quad b(s, w) = O(\|w\|^2),$$

and, differentiating this Taylor representation with respect to s and w ,

$$(B.8) \quad \begin{aligned} D_s a(s, w) &= O(\|w\|^2), & D_w a(s, w) &= O(\|w\|), \\ D_s b(s, w) &= O(\|w\|^2), & D_w b(s, w) &= O(\|w\|), \end{aligned}$$

and, for the second derivatives,

$$(B.9) \quad \begin{aligned} D_s^2 a(s, w) &= O(\|w\|), & D_s D_w a(s, w) &= O(\|w\|), & D_w^2 a(s, w) &= O(1), \\ D_s^2 b(s, w) &= O(\|w\|), & D_s D_w b(s, w) &= O(\|w\|), & D_w^2 b(s, w) &= O(1). \end{aligned}$$

All estimates are local and uniform. The weaker $O(\|w\|)$ estimate for $D_s^2 a$ and $D_s^2 b$ is sufficient for the argument below.

We already know from the proof of Theorem B.1 that

$$(B.10) \quad \|w_k\| \leq C \theta^k \|w_0\|, \quad \|D_z w_k\| \leq C \theta^k, \quad \sup_k \|D_z s_k\| \leq C.$$

We now control the second derivatives. Differentiating the recursions twice, and using (B.8)–(B.10), yields inequalities of the form

$$(B.11) \quad \|D_z^2 w_{k+1}\| \leq q \|D_z^2 w_k\| + C\theta^k (1 + \|D_z^2 s_k\| + \|D_z^2 w_k\|),$$

$$(B.12) \quad \|D_z^2 s_{k+1}\| \leq \|D_z^2 s_k\| + C\theta^k \|D_z^2 w_k\| + C\theta^{2k} (1 + \|D_z^2 s_k\|).$$

Indeed, (B.11) follows from the normal recursion $w_{k+1} = B_{s_k} w_k + b(s_k, w_k)$: the leading term is $B_{s_k} D_z^2 w_k$, while all remaining terms contain either a factor w_k , $D_z w_k$, or a coefficient of order $O(\|w_k\|)$. The estimate (B.12) is obtained similarly from the tangential recursion $s_{k+1} = s_k + a(s_k, w_k)$. By (B.11), since $q < \theta < 1$, a discrete Gronwall argument gives

$$\|D_z^2 w_k\| \leq C\theta^k \left(1 + \sup_{0 \leq j \leq k} \|D_z^2 s_j\| \right).$$

Substituting this estimate into (B.12), we obtain

$$1 + \sup_{0 \leq j \leq k+1} \|D_z^2 s_j\| \leq (1 + C\theta^{2k}) \left(1 + \sup_{0 \leq j \leq k} \|D_z^2 s_j\| \right).$$

Since $\sum_{k=0}^{\infty} \theta^{2k} < \infty$, another discrete Gronwall argument yields

$$(B.13) \quad \|D_z^2 w_k\| \leq C\theta^k, \quad \sup_k \|D_z^2 s_k\| \leq C.$$

We next show that the second derivative series of s_∞ converges uniformly. By the chain rule,

$$\begin{aligned} D_z^2(a(s_k, w_k)) &= D^2 a(s_k, w_k)[D_z(s_k, w_k), D_z(s_k, w_k)] \\ &\quad + Da(s_k, w_k)D_z^2(s_k, w_k). \end{aligned}$$

Using (B.8)–(B.13), each term on the right-hand side is bounded by $C\theta^k$. Hence

$$\|D_z^2(a(s_k, w_k))\| \leq C\theta^k,$$

and therefore

$$\sum_{k=0}^{\infty} D_z^2(a(s_k, w_k))$$

converges uniformly. The first derivative series already converges uniformly by Theorem B.1. Thus

$$s_\infty(s, w) = s + \sum_{k=0}^{\infty} a(s_k, w_k)$$

is C^2 , and consequently $\Psi_c(s, w) = (s_\infty(s, w), 0)$ is C^2 .

It remains to verify the second-order retraction property. From (B.3), (B.5), and (B.6), we have

$$s_\infty - s = \sum_{k=0}^{\infty} a(s_k, w_k) = O(\|w_0\|^2).$$

Since $s = P_X(z)$ and $\|w_0\| = \text{dist}(z, X)$, this gives

$$(B.14) \quad \Psi_c(z) = P_X(z) + O(\text{dist}(z, X)^2).$$

Now take $z = x + \xi$ with $x \in X$ and $\xi \in T_x X$. Since the intersection is clean and M is locally C^4 , the set $X = M \cap E$ is a C^4 embedded submanifold near \bar{x} . Hence

$$\text{dist}(x + \xi, X) = O(\|\xi\|^2),$$

and the metric projection retraction satisfies the standard expansion

$$P_X(x + \xi) = \text{Exp}_x(\xi) + O(\|\xi\|^3).$$

Combining this with (B.14), we obtain

$$R_x^c(\xi) = \Psi_c(x + \xi) = P_X(x + \xi) + O(\|\xi\|^4) = \text{Exp}_x(\xi) + O(\|\xi\|^3).$$

Since R^c is C^2 , this proves that R^c is a second-order retraction on X . □